CHAPTER 3.12

Testing and Calculations for Comminution Machines

Stephen Morrell

This chapter deals with the testing of rocks to determine their hardness/strength and the subsequent use of the test results in calculations that, in design, lead to the choice of an appropriately sized comminution machine. The equipment and flowsheet selection processes are discussed in the relevant chapters of this handbook. The usual calculation route to choose the comminution machine incorporates the following steps:

1. Rock samples are laboratory tested to obtain hardness parameter values.
2. An equation (or equations) that uses the hardness parameter values is applied to estimate the full-scale machine specific energy (kilowatt-hours per metric ton).
3. Given the required throughput capacity (metric tons per hour) of the comminution machine, its required power draw is estimated by multiplying the specific energy by the throughput capacity. Contingencies (safety factors) are then applied to this power draw.
4. A comminution machine is chosen that can deliver the required power. In the case of milling, this step requires the application of equations that relate dimensions and operating conditions to power draw (power model) so that the correct size of mill is chosen.

It follows from the preceding steps that a laboratory rock hardness test is of little value without an associated equation(s) that enables the prediction of the comminution machine specific energy. Also, it is paramount that the resultant predictions are accurate. For this to be established, extensive benchmarking is required in which predictions are compared with actual (observed) values from a wide range of operating full-scale plants.

In the following sections, several laboratory rock hardness testing methods will be described together with their associated specific energy equations. An overview of commonly used hardness test methods is provided in Table 1. The final section of this chapter will address tumbling mill power draw modeling.

Stirred mills are not included in this chapter, although are reviewed in Chapter 3.11, "Grinding Technologies." Their testing procedures and associated scale-up techniques and equipment sizing are specific to vendors and their particular mill design.

BOND

Fred C. Bond was the first person to develop laboratory tests and associated equations that could be applied to practical design situations. Interestingly, Bond never published any data to support the validity of his approach, though Blaskett (1969), Rowland (1973), and Moore (1982) did. Bond did conduct experiments on a larger scale to collect data with which he could test and tune at least some of his equations. However, the following quote from his 1961 Allis-Chalmers publication indicates that perhaps not all of his equations were rigorously derived from data: "Many (equations) are empirical, with numerous constants being derived from experience."

Bond's approach covers conventional crushers, and rod and ball mills. However, in his day, autogenous grinding and semiautogenous grinding (AG/SAG) mills and high-pressure grinding rolls (HPGRs) were not common or not yet invented, and hence his approach does not explicitly encompass these machines. Proprietary techniques, however, have been developed that have adapted his equations for use with AG/SAG mills, and some of these are described in the following sections.

Bond Laboratory Tests

Bond developed three laboratory rock characterization test procedures, each one associated with a particular comminution machine (i.e., crushers, rod mills, and ball mills). All the tests require relatively small amounts of material and hence are readily suited for use with drill core samples, as proposed in Table 1. However, ideally the crushing test needs whole PQ core. This tends to be less common (and more expensive) than NQ and HQ cores, which are suitable for use in Bond's rod and ball mill tests.

Crushing Test

For crushing applications, Bond developed an apparatus comprising two opposing 30-lb hammers that came together through the action of two counterrotating wheels (Bond 1946,

Stephen Morrell, President, SMC Testing Pty Ltd., Brisbane, Queensland, Australia

Table 1 Laboratory tests for comminution circuit design

Test	Use	References	Sample Quantity, kg	Material Size	Minimum Core Size
Bond impact crushing test	Conventional crushers	Bond 1946, 1961	40–50	2–3 in.	PQ
	SAG mills	Barratt and Allan 1986			
Bond rod mill work index	Rod mills / ball mills	Bond and Maxon 1943; Bond 1961; Rowland 1982	10–15	100% – 12.7 mm	NQ
	SAG mills	Barratt and Allan 1986			
Bond ball mill work index	Ball mills	Bond and Maxon 1943; Bond 1961; Rowland 1982	15	100% – 3.35 mm	NQ
	SAG mills	Barratt and Allan 1986			
Bond abrasion index	Wear prediction for crushers and tumbling mills	Bond 1963; Giblett and Seidel 2011	2	12–19 mm	NQ
SMC Test	Conventional crushers, AG/SAG mills, HPGRs	Morrell 2004a–c, 2009	20	19–31 mm	NQ
JK drop weight test	SAG mills, conventional crushers	Napier-Munn et al. 1996	75	13.2–63 mm	PQ
SPI Test	SAG mills	Starkey et al. 1994	10	80% – 12.7 mm	NQ
SAGDesign test	SAG mills	Starkey and Larbi 2012	15	80% – 19 mm	NQ

Source: Giblett and Morrell 2016

1961). The hammers were made of steel with a Brinnell hardness of 230. Each hammer was 2 in. in cross section and 28 in. long. The hammers were mounted on the wheels so their centers at rest were 16 in. below the axis of rotation of the wheels. The wheels were 22-in. front bicycle wheels, reinforced with steel bands around each rim. The left-hand wheel was initially rotated clockwise and, through a connecting device, the right-hand wheel was synchronized and rotated counterclockwise by a similar amount. As the hammers were attached to the wheels, the hammers were lifted up by this rotation, and when the wheels were released, the hammers would collide with one another at the 6 o'clock position. By measuring how high the hammers were raised in relation to their final rest position, the potential energy could be estimated. A rock specimen was mounted on a plinth at the point of collision of the hammers and hence was broken with an amount of energy equivalent to the estimated potential energy. Figure 1, taken from a modern machine that is faithful to Bond's original design, shows where the hammers collide.

Bond specified that only particles in the size range of –3 in. + 2 in. should be tested in this machine. Particles outside of this range should not be used. Bond (1946) also stated that slabby or acicular pieces should not be used. He recommended that a minimum of 10 suitable rocks should be broken. Mounting of the rocks was to follow this procedure: "If the longest dimension is designated as A, the longest dimension perpendicular to A as B and the longest dimension perpendicular to both A and B as C; the specimen is placed in the holder in such a position that the hammers strike on both sides of dimension C." For breaking each specimen, Bond (1946) quoted the following procedure: "The first piece is tested with a low-energy blow and the height of fall is gradually increased until the specimen breaks into two or more pieces of approximately equal size. Each succeeding piece is first tested with an energy slightly under that required to break the preceding piece and the height of fall is increased so that the specimen is broken after two or three blows." The aim of the test is therefore to try to measure the energy needed to just break the rock. The so-called crushing work index (W_{iC}) is then calculated using Equation 1, based on the average result from the 10 rocks.

Courtesy of Amdel Mineral Laboratories

Figure 1 Region where breakage takes place in Bond's crushing work index machine

$$W_{iC} = 2.85C/sg \quad \textbf{(EQ 1)}$$

where

W_{iC} = crushing work index, kW·h/t
C = E/D
E = breakage energy, ft-lb
D = rock thickness, in.
sg = specific gravity

Recently, some laboratories have started to use a machine with a design different from that developed by Bond (Figure 2). Experience has shown that machine design influences the outcome of breakage testing devices, and some data have suggested that this machine may not give the same results as Bond's original design (Bailey et al. 2009). Caution should

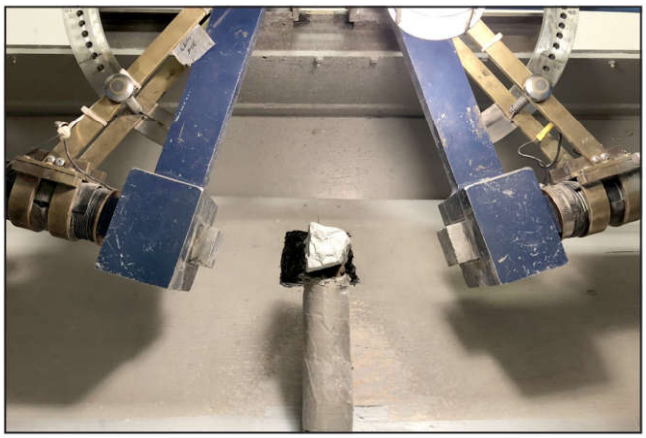

Reprinted with the permission of FLSmidth A/S

Figure 2 Modern version of Bond's crushing work index machine

Courtesy of JKTech Pty Ltd.

Figure 3 Bond rod mill

therefore be exercised if tests are conducted on machines that are not entirely faithful to Bond's original design.

Rod Milling Test

For rod milling, Bond (1961) developed a dry locked-cycle test that uses a 12-in.-diameter, 24-in.-long batch mill with wave liners and running at 46 rpm (see Figure 3). The mill is mounted on a rocker, which allows for the mill to be tilted up by 5° to the horizontal and down by 5°. The mill is charged with a specified quantity of rods of given sizes. The rock being characterized is stage-crushed to 100% passing 12.7 mm and ground, dry, in closed circuit with a screen of aperture P_1 such that the recycle load is 100%. Depending on the size of the starting material, stage crushing may need to involve an initial relatively coarse crush of the sample using a crusher setting of about 25 mm. The crusher is then set to 12–15 mm and the sample is passed through, with the product screened on a 12.7-mm sieve. The screen oversize is then passed again through the crusher, screened again at 12.7 mm, and so on, until the entire sample has passed through the 12.7-mm sieve. The net grams of final product produced when the recycle load is 100% is measured and inserted into Equation 2 to obtain the rod mill work index, W_{iR}. By inserting this value into Equation 4, Bond claimed that the specific energy of a wet 8-ft overflow rod mill in open circuit could be obtained.

Courtesy of BICO Braun International

Figure 4 Bond ball mill

$$W_{iR} = \frac{68}{P_1^{0.23}\,(\mathrm{Grp})^{0.625}\,10\left(\frac{1}{\sqrt{P}} - \frac{1}{\sqrt{F}}\right)} \qquad \textbf{(EQ 2)}$$

where

W_{iR} = bond laboratory rod work index, kW·h/t
P_1 = closing screen size, µm
Grp = net grams of screen undersize per mill revolution
P = 80% passing size of the product, µm
F = 80% passing size of the feed, µm

Ball Milling Test

For ball milling, Bond (1961) developed a dry locked-cycle test that uses a 12-in.-diameter, 12-in.-long batch mill with rounded corners and smooth liners and running at 70 rpm (see Figure 4). The mill is charged with a specified quantity of balls of given sizes. The rock being characterized is stage-crushed to 100% passing 3.35 mm and ground, dry, in closed circuit with a screen of aperture P_1 such that the recycle load is 250%. Depending on the size of the starting material, stage crushing may need to involve an initial relatively coarse crush of the sample using a crusher setting of about 25 mm. The crusher is then set to 3–4 mm and the sample is passed through, with the product screened on a 3.36-mm sieve. The screen oversize is then passed again through the crusher, screened again at 3.36 mm, and so on, until the entire sample has passed through the 3.36-mm sieve. The net grams of final product produced when the recycle load is 250% is measured and inserted into Equation 3 to obtain the ball mill work index. By inserting this value into Equation 4, Bond claimed that the specific energy of a wet 8-ft overflow ball mill in closed circuit could be obtained. Bond recommended that the screen aperture (P_1)

chosen to close the test with should be such that it gives a final product P_{80} similar to that being targeted in the full-scale plant. Typically, the final product P_{80} is of the order of $1/\sqrt{2}$ of the closing screen aperture.

$$W_{iB} = \frac{49}{P_1^{0.23}(Gbp)^{0.82}10\left(\frac{1}{\sqrt{P}} - \frac{1}{\sqrt{F}}\right)} \quad \textbf{(EQ 3)}$$

where W_{iB} is the Bond laboratory ball work index, in kW·h/t.

General Equations

Bond's general equation to predict the specific energy requirement for crushers, rod mills, and ball mills to reduce a feed with a specified F_{80} to a product with a specified P_{80} is as follows (Bond 1952):

$$W = 10W_i\,(P^{-0.5} - F^{-0.5}) \quad \textbf{(EQ 4)}$$

where

W = specific motor output energy, kW·h/t
W_i = work index, kW·h/t, as determined from the relevant laboratory test

Bond (1952) stated that Equation 4 "… conforms with the motor output power to an average overflow ball mill of 8 ft interior diameter grinding wet in closed circuit…."

Having developed Equation 4, Bond proceeded to modify it with a range of efficiency factors (EFs) that attempted to address the differences in feed and operating conditions of different circuit designs and ore types. These EFs applied to rod and ball mill circuits only. Using Rowland and Kjos's (1978) description, the EFs are as follows:

EF1—Dry grinding (rod and ball mills):
EF1 = 1.3 for dry grinding

EF2—Open-circuit milling (ball mills only):
EF2 = 1.2 for open-circuit grinding

EF3—Mill diameter (rod and ball mills):

$$EF3 = (8/D)^{0.2} \quad \textbf{(EQ 5)}$$

where D is the mill diameter, in ft, inside liners.

The diameter factor (see Equation 5) is particularly interesting (and much debated). Bond introduced it because of what he stated was an improvement in mill energy efficiency as the diameter increased above 8 ft. However, his argument as to the reason for this improvement is tenuous, to say the least, as it is based on his assertion in his 1961 paper that mill power draw increases on the basis of Diameter$^{2.4}$ and throughput capacity increases on the basis of Diameter$^{2.6}$. He concluded that the difference in these diameter exponents of 2.6 and 2.4 was 0.2, and this meant that the kilowatt-hours per ton required to grind decreases on the basis of Diameter$^{0.2}$. Interestingly, in 1962 Bond changed his mill power draw exponent from 2.4 to 2.3 but did not change his diameter efficient factor to 0.3, as would be expected from his arguments.

Rowland (1972) modified the application of EF3 and stated that it should be used in mills up to 12.5 ft and then kept at the 12.5-ft value for all larger mills (i.e., EF3 = 0.914 for mills larger than 12.5-ft diameter). The capacity problems experienced by Bougainville Copper (Steane and Hinckfuss 1979) brought into review the efficiency of larger mills, and at the time, some placed blame on the size of the mill, as it was one of the biggest diameter mills of its day (18 ft). This led to the belief by some that mills with larger diameters were in fact less efficient than smaller ones, in direct contrast to Bond's assertion. However, by 1988, ball mills had reached 21 ft with no apparent diameter-related problems (Forsund et al. 1988). Most likely, there is no change in the energy efficiency of mills as they increase in diameter, as Morrell (2001) demonstrated using data from a range of mill sizes. This finding is confirmed by the data in Figure 5, which shows the results of predicting ball mill specific energy using the Bond ball mill work index and Bond's equation (with no correction factors). The figure shows the error of the predicted specific energy as compared to the observed values from 45 operating ball mills with diameters in the range of 12 to 26 ft. If diameter did influence the specific energy efficiency, then there should be a significant trend in the error with respect to mill diameter, hence suggesting that a diameter efficiency factor is warranted. This is not apparent in the data, and therefore the hypothesis that mill diameter influences energy efficiency is not supported, at least within the range of 12 to 26 ft.

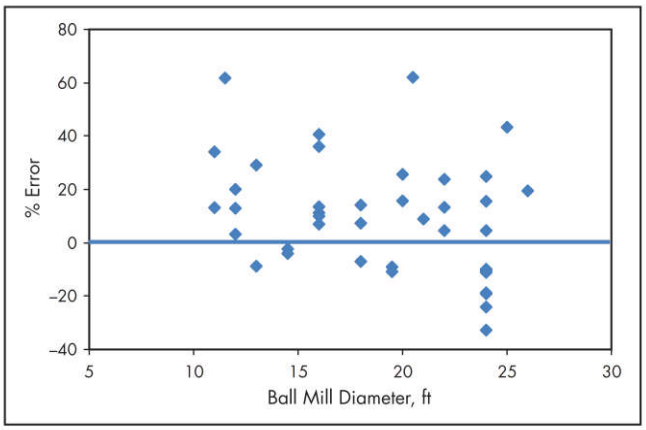

Figure 5 Observed error in ball mill specific energy using Bond's equation versus mill diameter

EF4—Oversize feed (rod and ball mills):

$$EF4 = (R_r + (W_i/1.1 - 7) \times ((F_{80} - F_o)/F_o))/R_r \quad \textbf{(EQ 6)}$$

where

R_r = reduction ratio F_{80}/P_{80}
$F_o = 16{,}000 \times (14.3/W_i)^{0.5}$ for rod milling circuits **(EQ 7)**
$= 4{,}000 \times (14.3/W_i)^{0.5}$ for ball milling circuits **(EQ 8)**
W_i = bond laboratory work index, in kW·h/t; use rod mill work index for rod milling circuits and ball mill work index for ball mill circuits

applied only where $F_o < F_{80}$.

EF5—Fineness of grind (ball mills only):

$$EF5 = (P_{80} + 10.3)/(1.145 \times P_{80}) \quad \textbf{(EQ 9)}$$

applied when grinding finer than a P_{80} of 75 µm.

EF6—High or low reduction ratio (rod milling only):

$$EF6 = 1 + (R_r - R_{ro})^2/150 \quad \textbf{(EQ 10)}$$

where

R_r = reduction ratio F_{80}/P_{80}

$$R_{ro} = 8 + 5L/D \quad \textbf{(EQ 11)}$$

L = rod length
D = mill diameter

applied only when R_r falls outside of the range $R_{ro} \pm 2$.

EF7—Low reduction ratio (ball milling only):

$$EF7 = (2 \times (R_r - 1.35) + 0.26)/(2 \times (R_r - 1.35)) \quad \textbf{(EQ 12)}$$

where R_r is the reduction ratio F_{80}/P_{80}—applied only when R_r is less than 6.

EF8—Rod mill feed size distribution (rod mills only):

EF8 = 1.4 in rod-mill-only circuits fed with feed from an open crushing circuit
= 1.2 in rod-mill-only circuits fed with feed from a closed crushing circuit
= 1.2 in rod-mill-only circuits fed with feed from an open crushing circuit
= 1.0 in rod-mill-only circuits fed with feed from a closed crushing circuit

Equation Accuracy

Rod and Ball Mills

Unfortunately, there is little published data on the accuracy of Bond's original equations or the modifications to them that Rowland (1972) subsequently introduced. Blaskett (1969) provided some relevant data for relatively small ball mills in the diameter range of 5 to 10.5 ft, and Rowland (1973) also published some data on rod mills in the range of 9 to 12 ft and ball mills in the range of 9 to 19.5 ft. These data are shown in Figure 6. The Blaskett ball mill results indicate one data set in particular that has problems. This data set comes from a primary ball mill grinding from 11.6 mm to a relatively coarse 630 µm. The resultant EF4 (coarse grinding factor) was an extremely large 2.35, and hence the predicted power requirement was also relatively large and did not match the relatively small energy requirement observed in the plant. If the mill had been grinding to a much finer 150 µm, for example, the associated EF4 factor would be only 1.3, which seems counterintuitive, as it suggests that the mill would become more energy efficient if it were to grind finer. It is possible, therefore, that there is a problem with the EF4 factor where the grind is relatively coarse.

If Rowland's data only in Figure 6 are considered, the standard deviation of the differences between observed and predicted specific energies is 9.3% with a mean difference of 1.8%. If Blaskett's data are added (and ignoring the one problematic data set), this standard deviation increases to 25.6% with an overall mean of differences of 16.5%.

In the case of the rod mill data, the standard deviation of the differences between observed and predicted specific energies is 12.6% with an overall mean of differences of 21.8%.

Crushing

In the case of crushing, Moore (1982) published several data sets that show the approach has very poor accuracy (see Figure 7) and confirms Flavel and Rimmer's (1981) similar conclusions from a study they conducted while working for Allis-Chalmers (where Bond worked when he originally developed the test). Flavel and Rimmer claimed that the reason for the inaccuracy was that Bond originally developed his

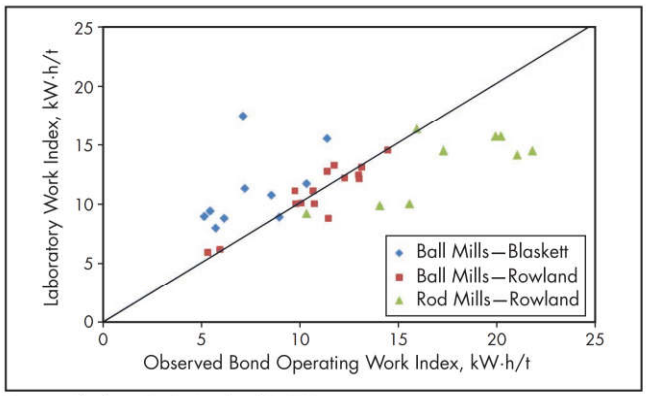

Source: Blaskett 1969; Rowland 1973

Figure 6 Bond laboratory rod and ball mill work index versus observed operating work index

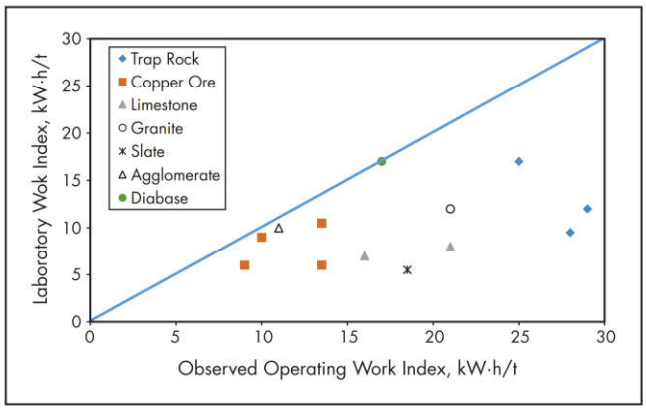

Source: Moore 1982

Figure 7 Bond laboratory crushing work index versus observed operating crushing work index

crushing work index test for primary crushers in which the applied specific energy is low (~0.1 kW·h/t), but it was not suitable for secondary and tertiary crushers where the applied specific energy was much higher (>0.25 kW·h/t). A contributing cause is the inherent very poor reproducibility of the test as reported by Angove and Dunne (1997) in a study they conducted in which three different samples were sent to several laboratories for Bond crushing work index testing. Results indicated a huge variation in work index values, with maximum values consistently almost double the minimum values. This variation is suspected to be caused by both the lack of standardization in equipment used by different laboratories and the operator sensitivity inherent in the use of the machine.

Analysis of the data in Figure 7 indicates that the standard deviation of the differences between observed and predicted values is 22.9% with an overall mean of differences of 39.9%.

Equipment and Procedural Considerations with Bond Tests

Several factors should be addressed when conducting Bond tests to ensure that the most accurate and repeatable results are obtained. These factors can be divided into two principal categories: (1) those related to the equipment and (2) those related to how the tests are conducted.

Equipment factors relate to the design/operation of the equipment. Hence the equipment being used should conform to Bond's specification. A check of the following should help ensure that the most important specifications have been met:

- Crushing tester generally conforms to the design in Figure 1.
- Crushing hammers are the correct mass and shape, and made of the specified material (hardness).
- Ball/rod mill dimensions are correct.
- Rotational speeds are correct.
- Rods are the correct sizes and weight/number per size class.
- Balls are the correct sizes and weight/number per size class.
- Ball mill has curved edges and an access door that closes flush with the inside of the mill.
- Rod mill has liners, and these are the correct thickness and shape.
- Ball mill has no liners.
- Rod mill has a rocker system to allow for the mill to be tilted by 5° up and down.

In terms of how the rod and ball mill tests should be conducted, Mosher and Tague (2001) provide particularly good guidance. Based on their advice and other experience, checking the following should ensure good operational procedures:

- Crushing work index rock specimens must be in the size range of 2 to 3 in.
- Ball mill closing screen aperture (P_1) has been chosen such that it gives a final product P_{80} similar to that being targeted in the full-scale plant. Typically, the final product P_{80} is of the order of $1/\sqrt{2}$ of the closing screen aperture.
- Feed samples have been generated by riffling from the master sample that has been correctly stage-crushed. Depending on the size of the starting material, this may need to involve an initial relatively coarse crush of the sample using a crusher setting of about 25 mm. The crusher is then set to just over the top size required for the test and the sample is passed through, with the product being screened on the required sieve. The screen oversize is then passed again through the crusher, screened again on the sieve, and so on, until the entire sample has passed through the sieve.
- Sizing of feed and products has been done on a full set of fourth root of two sieves to ensure accurate measurement of the F_{80} and P_{80}.
- The final three cycles have shown a reversal in the Grp/Gbp trend and are within 3% of one another.

Worked Examples

The following worked examples have been taken from Rowland and Kjos (1978) to illustrate the application of Bond's approach. The following Bond test data are provided:

- Rod work index = 14.52 kW·h/t
- Ball work index = 12.87 kW·h/t at a closing screen size of 250 µm

Two circuits are considered, a rod mill–ball mill circuit and a single-stage ball mill circuit fed from a crushing circuit, both with a final product size P_{80} of 175 µm. The examples consider the determination of the milling circuit specific energy.

Rod Mill–Ball Mill Circuit

Rowland and Kjos (1978) specified that the rod mill would be fed from a closed-circuit crushing plant producing a P_{80} of 18 mm and further specified that the rod mill would grind to a P_{80} of 1,200 µm. Considering the rod mill circuit:

$$W = 10 \times 14.52 \times (1{,}200^{-0.5} - 18{,}000^{-0.5}) \text{ kW·h/t (uncorrected)}$$
$$= 3.11 \text{ kW·h/t}$$

EF1, EF2, EF5, EF7, and EF8 do not immediately apply. EF3 and EF6 need to be determined after a mill size has been selected (see later), leaving EF4 to be determined at this stage.

$$R_r = 18{,}000/1{,}200 = 15$$

$$F_o = 16{,}000 \times (14.3/14.52)^{0.5} = 15{,}878$$

As $F_o < 18{,}000$, then EF4 is applied:

$$EF4 = \left(15 + \left(\frac{14.52}{1.1}\right) - 7\right) \times \frac{\left(\frac{18{,}000 - 15{,}878}{15{,}878}\right)}{15}$$
$$= 1.06$$

Rowland and Kjos select 11.35-ft-diameter mills inside liners, and hence for EF3:

$$EF3 = (8/11.35)^{0.2} = 0.93$$

They then select 17-ft-long mills using 16.5-ft rods. Hence, evaluating EF6:

$$R_{ro} = 8 + 5 \times 16.5/11.35 = 15.3$$

As this value is within the limits $R_r \pm 2$ (15 ± 2), EF6 does not apply. The final (corrected) rod mill specific energy is given by

$$\text{specific energy} = W \times EF3 \times EF4$$
$$= 3.11 \times 0.93 \times 1.06 \text{ kW·h/t}$$
$$= 3.07 \text{ kW·h/t}$$

For the ball mill circuit: The ball mill circuit feed is the product of the rod mill, and hence the ball mill F_{80} is 1,200 µm. The target product P_{80} is 175 µm and hence,

$$W = 10 \times 12.87 \times (175^{-0.5} - 1{,}200^{-0.5}) \text{ kW·h/t (uncorrected)}$$
$$= 6.01 \text{ kW·h/t}$$

Efficiency factors EF1, EF2, EF5, EF6, EF7, and EF8 do not apply.

Rowland and Kjos chose a mill with a diameter greater than 12.5 ft, so EF3 applies but is fixed at 0.914. The application of EF4 has to be evaluated by reference to F_o. Hence,

$$F_o = 4{,}000 \times (14.3/12.87)^{0.5} = 4{,}216 \text{ µm}$$

As $F_o > 1{,}200$, then EF4 is not applied. The final (corrected) ball mill specific energy is then given by

$$\text{specific energy} = W \times EF3$$
$$= 6.01 \times 0.914 \text{ kW·h/t}$$
$$= 5.5 \text{ kW·h/t}$$

Single-Stage Ball Mill Circuit

Rowland and Kjos (1978) specified for this worked example that the ball mill would be fed by a closed-circuit crusher producing a product with a P_{80} of 9.4 mm, and hence the ball mill circuit F_{80} would be 9,400 µm. Rowland (1972) asserts that in cases where the ball mill circuit receives coarser feed, some of which is larger than 3.35 mm (top size in the Bond ball mill work index test), for this fraction the rod mill work index is more relevant. In such cases, he therefore divides the ball mill specific energy calculation into two steps. The first step uses the rod mill work index from the ball mill circuit F_{80} down to 2,100 µm, while the second step applies the ball mill work index from 2,100 µm down to the final grind. Hence,

Step 1

$$W = 10 \times 14.52 \times (2{,}100^{-0.5} - 9{,}400^{-0.5})\ \text{kW·h/t}$$
(uncorrected)
$$= 1.67\ \text{kW·h/t}$$

Step 2

$$W = 10 \times 12.87 \times (175^{-0.5} - 2{,}100^{-0.5})\ \text{kW·h/t}$$
(uncorrected)
$$= 6.92\ \text{kW·h/t}$$

This totals 8.59 kW·h/t. The efficiency factors EF1, EF2, EF5, EF6, EF7, and EF8 do not apply.

Rowland and Kjos chose a mill with a diameter greater than 12.5 ft, so EF3 applies but is fixed at 0.914. The application of EF4 must be evaluated by reference to F_o. Hence

$$F_o = 4{,}000 \times (14.3/14.52)^{0.5}$$
(note that the rod mill work index is used in this case)
$$= 3{,}970\ \mu\text{m}$$

As $F_o < 9{,}400$, then EF4 is applied.

$$R_r = 9{,}400/175 = 53.7$$

$$EF4 = (53.7 + (12.87/1.1 - 7) \times ((9{,}400 - 3{,}970)/3{,}970))/53.7 = 1.12$$

The final (corrected) ball mill specific energy is then given by

$$\text{specific energy} = W \times EF3 \times EF4$$
$$= 8.59 \times 0.914 \times 1.12\ \text{kW·h/t}$$
$$= 8.79\ \text{kW·h/t}$$

BOND TESTS FOR AG/SAG CIRCUITS

Bond did not specifically develop tests for predicting the specific energy of AG/SAG circuits. However, over the years, some have attempted to adapt his techniques to overcome this deficiency. One such approach was developed by Barratt and Allan (1986) in which they used a combination of the standard Bond crushing, rod mill, and ball mill work index tests.

Equations

The equation Barratt and Allan (1986) developed for AG/SAG mill circuits is as follows:

$$E_{SAG} = 1.25 \cdot [(10 \cdot W_{iC} (P_C^{-0.5} - F_C^{-0.5})) + (10 \cdot W_{iR} (P_R^{-0.5} - F_R^{-0.5}) \cdot K_R) + (10 \cdot W_{iB} (110^{-0.5} - F_B^{-0.5}) \cdot K_B)] - (10\, W_{iB} (110^{-0.5} - T_{SAG}^{-0.5}) \cdot K_B) \quad \textbf{(EQ 13)}$$

The equation for the associated ball mill circuit is

$$E_{BM} = 10 \cdot W_{iB} (P_B^{-0.5} - T_{SAG}^{-0.5})\, K_B \quad \textbf{(EQ 14)}$$

where

E_{SAG} = specific energy of the SAG mill circuit
E_{BM} = specific energy of the ball mill circuit
W_{iC}, W_{iR}, W_{iB} = bond crushing, rod, and ball work indices, respectively
P_C, P_R, P_B = 80% passing size of the product of the stage associated with crushing, rod milling, and ball milling, respectively
F_C, F_R, F_B = 80% passing size of the feed of the stage associated with crushing, rod milling, and ball milling, respectively
K_R = composite of the rod mill (EF) factors (Rowland 1982), excluding the diameter factor
K_B = composite of the ball mill (EF) factors (Rowland 1982), excluding the diameter factor
T_{SAG} = transfer size (80% passing) between the AG/SAG and ball mill circuits

All P and F values as well as the T_{SAG} must be specified/estimated for Equations 13 and 14 to be applied. The value used for T_{SAG} was recognized by Barratt and Allan (1986) as critical to the prediction of the SAG mill circuit specific energy (and by inference also the ball mill circuit specific energy).

Validation

While the method has been used in support of grinding circuit design and optimization on several projects, no definitive published validation data on the method is available yet.

MORRELL

Morrell, like Bond, also developed ore characterization tests (Morrell 2004a) as well as associated equations (Morrell 2004a, 2009, 2010). These enabled the application of the test results in design situations using both power-based equations and simulation modeling. In the course of development, Morrell collected large quantities of operational plant data with which to ensure the validity and accuracy of his approach. Unlike Bond's approach, which does not explicitly cover AG/SAG and HPGR circuits, Morrell's approach does.

Morrell Laboratory Tests

Morrell developed one new laboratory test, the SMC Test, which covers the size reduction in crushers, HPGRs, rod mills, and AG/SAG mills, and adapted Bond's ball mill laboratory work index test to cover ball mills.

SMC Test

The SMC Test was developed by Morrell to provide a range of comminution parameters from the breakage of relatively small amounts of small-diameter drill core. SMC is an acronym for Steve Morrell comminution (not SAG mill comminution as is incorrectly stated in some published literature). SMC Testing Pty Ltd. currently owns the SMC Test.

Normally, 15–20 kg of drill core (or rocks) are required by the laboratory to conduct the test (though under some conditions, much less can be used), from which 1–5 kg is extracted for the actual test depending on the size fraction chosen to do the test with. This material can be added back to the original sample and reused to conduct a standard Bond ball work index test.

The test uses the JK drop weight testing device to break a suite of 100 closely sized particles at five different energy levels. The particle size used for the test is chosen from one of the following three fractions: –31.5 + 26.5 mm, –22.4 + 19 mm, or –16 + 13.2 mm. The choice of which size fraction to use depends on the source material; for example, if only quartered (slivered) BQ (38 mm) core is available, then the smallest size fraction would be chosen, while if larger diameter core were available, then the coarser size fractions could be used. In general, where sample size/quantity permits, the largest size fraction should be used.

The particles for the test can be obtained using two different feed preparation routes. If a relatively small quantity of drill core sample is available (i.e., much less than the usual 15–20 kg required), then the particles can be produced by cutting the drill core into wedges (Figure 8). If sample quantity is not a problem, then the particles are produced by "light" stage-crushing of the core and selecting the required sizes via sieving the product at the end of each stage (Figure 9). Light stage-crushing involves crushing the drill core in stages, with each successive stage having a smaller gap setting and the gap settings chosen so that the reduction ratios (F_{80}/P_{80}) of each stage are relatively small. This ensures that the maximum amount of correct sized particles is produced and at the same time minimizes the amount of fines produced. Research has shown that there is no difference in results from using either diamond-cut or crushed material (see www.smctesting.com/about/technical-information).

The raw data from the SMC Test is processed, and from the results a range of comminution parameters are generated. These parameters fall into two groups. The first group contains parameters that are used in power-based equations for predicting the specific energy of comminution machines. This group includes the comminution indices DW_i, M_{ia}, M_{ih}, and M_{ic}. They cover the following circuits:

1. AG and SAG mills
2. Rod mills
3. Crushers
4. HPGRs

The second group contains parameters that are used for simulation modeling purposes, notably the AG/SAG and crusher models used in the comminution simulator JKSimMet. This group includes the JK rock breakage parameters A, b, and t_a as well as the JK crusher model's t10-Ecs matrix.

When the SMC Test is conducted using relatively small particle sizes (i.e., 14 mm or 20 mm), it may be necessary to confirm the size-adjustment factor that the SMC Test data processing algorithm uses to estimate the A and b parameters for these particle sizes. When 28-mm particles have been used, a size-adjustment factor is not required. The size-adjustment necessary when 14-mm or 20-mm particles are used is typically referred to as *calibration*. The need for such a factor arises from the change in rock hardness that is observed in all rocks as the particle size changes. This change is reflected in the change in the magnitude of the A*b parameter with size that can be observed from the data obtained in a drop weight test. The gradient of this A*b variation with size is determined from a drop weight test. It is used to "calibrate" the SMC Test A and b estimation algorithm, which then estimates the magnitude of the appropriate size-adjustment factor. The average particle size tested in a drop weight test is ~28 mm, and hence, the drop weight test A and b values relate on average to breakage of this particle size. The purpose of the SMC Test size-adjustment algorithm is, through the use the A*b-size gradient, to determine the amount of adjustment to the raw SMC Test results such that they reflect breakage of 28-mm particles (i.e., breakage of the average particle size of the drop weight test). As mentioned earlier, if the SMC Test has been conducted using 28-mm particles in the first instance, little to no size adjustment is necessary (i.e., the size-adjustment factor tends to unity), as this is the same size as the average particle tested in a drop weight test. Note that calibration only applies to the estimation of A and b values and is not used in the generation of the power-based parameters DW_i, M_{ia}, M_{ic}, and M_{ih}.

If a drop weight test is not done in conjunction with a SMC Test, then calibration is conducted using factors obtained from SMC Testing's database of over 500 SMC Test–drop weight test pairs. These data show that most ores have a similar calibration factor and that A and b parameters generated

Courtesy of SMC Testing Pty Ltd.

Figure 8 Particles selected for SMC testing from cutting drill core

Courtesy of SMC Testing Pty Ltd.

Figure 9 Particles selected for SMC testing from crushed rock

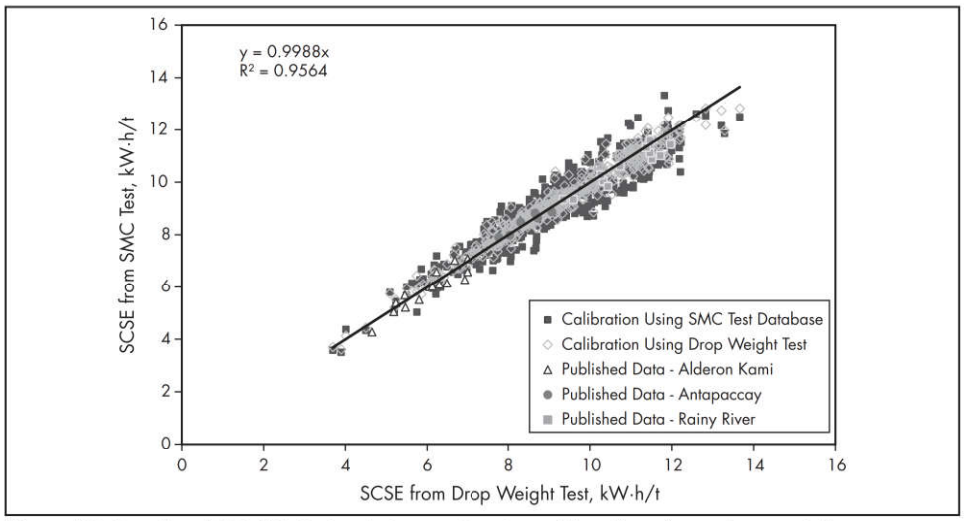

Figure 10 Results of AG/SAG simulations using A and b values from drop weight tests versus those from SMC Tests

from SMC Tests using the database calibration factors result in simulation results similar to those obtained using full drop weight tests or results from processing SMC Tests using calibration factors obtained from associated drop weight tests (see Figure 10). Figure 10 also includes some results based on data from several projects in the public domain to further illustrate this point. The data in this figure relate to the standard circuit specific energy (SCSE) parameter (Matei et al. 2015). The SCSE was adopted by JKTech in 2015 to represent the value of A*b in units of kilowatt-hours per ton that would result from the use of A*b in the simulation of a defined (standard) SAG mill circuit. This approach was adopted for several reasons, including to remove the nonlinear relationship that exists between A*b and the resistance of a rock to breakage by impact. This last factor is particularly important when comparing the A*b values of different ore samples and gives rise to the somewhat counterintuitive phenomenon that the difference in hardness between two samples with A*b values of, for example, 25 and 29 (15% difference) may be statistically different from a specific energy perspective, yet in the case of two samples with A*b values of 250 and 350 (40% difference) they may not be significantly different. The only way to tell is through simulating the influence that the different A and b values have on the AG/SAG mill specific energy.

Statistical analysis of the data in Figure 10 shows that the standard deviation of the differences between the drop weight test SCSEs and the SMC Test SCSEs is 3.8% when calibration using drop weight test results is used and 6.2% when SMC Test database calibration is used. In both cases, the overall mean of differences is 0.0%. The recent extensive Round Robin program conducted by JKTech (Matei et al. 2015) showed that the repeatability of the drop weight test SCSE was 3.8% (one standard deviation). Comparing this result with the statistics of the data in Figure 10 suggests that when drop weight test calibration is employed, the SCSEs from the SMC Test are statistically indistinguishable from those of a drop weight test. If, instead, calibration is conducted using the database, the degree of uncertainty in the SCSE, as measured by the standard deviation, increases only by 2.4 percentage points.

Ball Mill Laboratory Test

Morrell's approach for ball milling takes the raw data from a standard Bond ball mill work index test and uses it to generate a ball mill parameter, M_{ib}, which is compatible with the SMC Test parameters, M_{ia}, M_{ic}, and M_{ih}. The equation to obtain the M_{ib} is as follows (Morrell 2009):

$$M_{ib} = \frac{18.18}{P_1^{0.295}(\text{Gbp})\left(P_{80}^{f(p_{80})} - F_{80}^{f(f_{80})}\right)} \quad \textbf{(EQ 15)}$$

where M_{ib} is the fine ore work index, in kW·h/t. Note that the test should be carried out with a closing screen size that gives a final product P_{80} similar to that intended for the full-scale circuit.

General Equations

From a study of many operating circuits, Morrell (2004b) developed the following general size-specific energy equation:

$$W_i = M_i 4\left(x_2^{f(x_2)} - x_1^{f(x_1)}\right) \quad \textbf{(EQ 16)}$$

where

W_i = specific comminution energy, kW·h/t
M_i = work index related to the breakage property of an ore, in kW·h/t, and the type of equipment used (e.g., tumbling mill, crusher, or HPGR)
x_2 = 80% passing size for the product, µm
x_1 = 80% passing size for the feed, µm

$$f(x_j) = -(0.295 + x_j/1{,}000{,}000); \quad j = 1,2 \text{ (Morrell 2009)} \quad \textbf{(EQ 17)}$$

For tumbling mills, the specific comminution energy (W_i) relates to the power at the pinion or, for gearless drives, the power at shell. For HPGRs it is the energy inputted to the rolls, while for conventional crushers W_i relates to the specific energy as determined using the motor input power, less the no-load power.

Equation 16 is used in conjunction with the following three equipment categories:

1. Tumbling mills (e.g., AG, SAG, rod, and ball mills). Size reduction specific energy is predicted using two indices: M_{ia} and M_{ib}.
2. Conventional reciprocating crushers (e.g., jaw, gyratory, and cone), which use one index: M_{ic}.
3. HPGRs, which use one index: M_{ih}.

For tumbling mills, the two indices relate to coarse and fine ore particle breakage properties. *Coarse* in this case is defined as spanning the size range from a P_{80} of 750 µm up to the P_{80} of the product of the last stage of crushing or HPGR size reduction prior to grinding. *Fine* covers the size range from a P_{80} of 750 µm down to P_{80} sizes typically reached by conventional ball milling (i.e., about 45 µm).

The work index covering grinding in tumbling mills of coarse sizes is labeled M_{ia}. The work index covering grinding of fine particles is labeled M_{ib} (Morrell 2009). M_{ia} values are provided as a standard output from an SMC Test, while M_{ib} values can be determined using the data generated by a conventional Bond ball mill work index test. Note that the M_{ib} is *not* the Bond ball work index. M_{ic} and M_{ih} values are also provided as a standard output from an SMC Test.

The total specific energy (W_T) to reduce in size primary crusher product to final product is given by

$$W_T = W_a + W_b + W_c + W_h + W_s \quad \textbf{(EQ 18)}$$

where
- W_a = specific energy to grind coarser particles in tumbling mills
- W_b = specific energy to grind finer particles in tumbling mills
- W_c = specific energy for conventional crushing
- W_h = specific energy for HPGRs
- W_s = specific energy correction for size distribution (crushing–ball mill circuits only)

Clearly, only the W values associated with the relevant equipment in the circuit being studied are included in Equation 18.

Tumbling Mills

For coarse particle grinding in tumbling mills, Equation 16 is written as

$$W_a = K_1 M_{ia} 4\left(x_2^{f(x_2)} - x_1^{f(x_1)}\right) \quad \textbf{(EQ 19)}$$

where
- K_1 = 1.0 for all circuits that do not contain a recycle pebble crusher and 0.95 where circuits do have a pebble crusher
- M_{ia} = coarse ore work index and is provided directly by SMC Test
- x_2 = 750 µm
- x_1 = P_{80}, of the product of the last stage of crushing before grinding, µm

For fine particle grinding, Equation 16 is written as

$$W_b = M_{ib} 4\left(x_3^{f(x_3)} - x_2^{f(x_2)}\right) \quad \textbf{(EQ 20)}$$

where
- M_{ib} = fine ore work index
- x_3 = P_{80} of final grind, µm
- x_2 = 750 µm

By combining Equations 19 and 20, the total specific energy of the tumbling mill circuit is predicted. In AG/SAG–ball mill circuits, if the specific energies of the AG/SAG mill and the ball mill are required separately, then an additional equation is required that predicts the AG/SAG mill specific energy. The ball mill specific energy is then found from the difference between this value and the total milling circuit specific energy.

The AG/SAG mill specific energy equation in general form is as follows (Morrell 2011a) and contains all of the variables that are known to influence AG/SAG mill specific energy:

$$S = K \cdot F_{80}^{a} \cdot DW_i^{b} \left(1 + c(1 - e^{-dJ})\right)^{-1} \phi^{e} \cdot f(A_r) \cdot g(x) \quad \textbf{(EQ 21)}$$

where
- S = specific energy at the pinion
- K = an empirical function whose value is dependent upon whether a pebble crusher is in-circuit and whether the crushed pebbles are returned to the SAG mill or sent directly to the ball mill
- F_{80} = 80% passing size of the feed
- DW_i = drop weight index (from the SMC Test)
- a, b, c, d, e, f, g = empirical constants
- J = volume of balls, %
- ϕ = mill speed, % of critical
- $f(A_r)$ = function of mill aspect ratio
- g(x) = function of trommel aperture

The empirical constants in Equation 21 were fitted to operating data from 70 different concentrators covering over 110 different ore types. Details of these constants are proprietary and are currently owned by CITIC SMCC Process Technology.

Conventional Crushers

Equation 16 for conventional crushers is written as

$$W_c = S_c K_2 M_{ic} 4\left(x_2^{f(x_2)} - x_1^{f(x_1)}\right) \quad \textbf{(EQ 22)}$$

where
- S_c = coarse ore hardness parameter, which is used in primary and secondary crushing situations. It is defined by Equation 23 with K_s set to 55.
- K_2 = 1.0 for all crushers operating in closed circuit with a classifying screen. If the crusher is in open circuit (e.g., pebble crusher in an AG/SAG circuit), K_2 takes the value of 1.19.
- M_{ic} = crushing ore work index and is provided directly by SMC Test
- x_2 = P_{80} of the circuit product, µm
- x_1 = P_{80} of the circuit feed, µm

The coarse ore hardness parameter (S) makes allowance for the decrease in ore hardness that becomes significant in relatively coarse crushing applications such as primary and secondary cone/gyratory circuits. In tertiary and pebble crushing circuits, it is normally not necessary and takes the value of unity. In full-scale HPGR circuits where feed sizes tend to be higher than used in laboratory and pilot-scale machines, the parameter has also been found to improve predictive accuracy. The parameter is defined by Equation 23 with K_s set to 35.

$$S = K_s (x_1 \cdot x_2)^{-0.2} \quad \textbf{(EQ 23)}$$

where

K_s = machine-specific constant that takes the value of 55 for conventional crushers and 35 in the case of HPGRs
x_1 = P_{80} of the circuit feed, µm
x_2 = P_{80} of the circuit product, µm

Note that the procedure to determine when the parameter S should be applied is to first use Equation 23 to determine the value of S, and if it is less than 1, then it should be applied. If it is greater than 1, it should be set at 1.0.

High-Pressure Grinding Roll

Equation 16 for an HPGR's crushers is written as

$$W_h = S_h K_3 M_{ih} 4\left(x_2^{f(x_2)} - x_1^{f(x_1)}\right) \quad \textbf{(EQ 24)}$$

where

S_h = coarse ore hardness parameter as defined by Equation 23 and with K_s set to 35, K_3 = 1.0 for all HPGRs operating in closed circuit with a classifying screen. If the HPGR is in open circuit, K_3 takes the value of 1.19.
M_{ih} = HPGR ore work index and is provided directly by SMC Test
x_2 = P_{80} of the circuit product, µm
x_1 = P_{80} of the circuit feed, µm

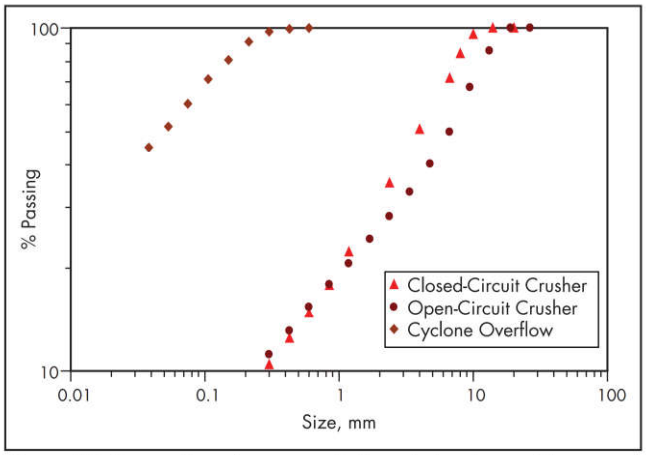

Figure 11 Examples of open and closed-circuit crushing distributions compared with a typical ball mill cyclone overflow distribution

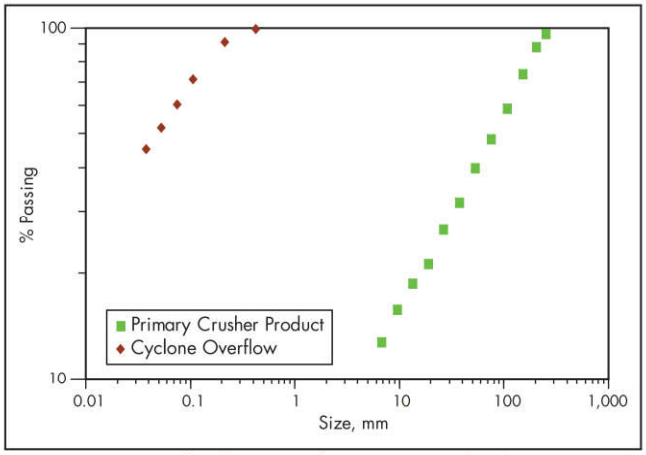

Figure 12 Example of a typical primary crusher (open circuit) product distribution compared with a typical ball mill cyclone overflow distribution

Specific Energy Correction for Size Distribution (W_s)

Implicit in the approach described in this section is that the feed and product size distributions are parallel and linear in log-log space. The same is true of Bond's approach (Bond 1960) and arises from the fact that the distributions are represented by a single point (the 80% passing size). Where they are not parallel, allowances (corrections) need to be made, a point also recognized by Bond (1961). Such corrections are most likely to be necessary (or are large enough to be warranted) when evaluating circuits in which closed-circuit secondary/tertiary crushing is followed by ball milling. This is because such crushing circuits tend to produce a product size distribution that is relatively steep when compared to the ball mill circuit cyclone overflow. This situation is illustrated in Figure 11, which shows measured distributions from an open and closed crusher circuit as well as a ball mill cyclone overflow. The closed-circuit crusher distribution is relatively steep compared with the open-circuit crusher distribution and ball mill cyclone overflow. Also, the open-circuit distribution more closely follows the gradient of the cyclone overflow. If a ball mill circuit were to be fed two distributions, each with same P_{80} but with the open- and closed-circuit gradients in Figure 11, the closed-circuit distribution would require more energy to grind to the final P_{80}. How much more energy is required is difficult to determine. However, it has been assumed that the additional specific energy for ball milling is the same as the difference in specific energy between open and closed crushing to reach the nominated ball mill feed size. This assumes that a crusher would provide this energy. However, in this situation the ball mill has to supply this energy and it has a different (higher) work index than the crusher (i.e., the ball mill is less energy efficient than a crusher and has to input more energy to do the same amount of size reduction). Hence from Equation 22, to crush to the ball mill circuit feed size (x_2) in open circuit requires specific energy equivalent to

$$W_c = 1.19 * M_{ic} 4\left(x_2^{f(x_2)} - x_1^{f(x_1)}\right) \quad \textbf{(EQ 25)}$$

For closed-circuit crushing, the specific energy is

$$W_c = 1 * M_{ic} 4\left(x_2^{f(x_2)} - x_1^{f(x_1)}\right) \quad \textbf{(EQ 26)}$$

The difference between the two (Equations 25 and 26) has to be provided by the milling circuit with an allowance for the fact that the ball mill, with its lower energy efficiency, has to provide it and not the crusher. This is what is referred to in Equation 18 as W_s and for the previous example is therefore represented by

$$W_s = 0.19 * M_{ia} 4\left(x_2^{f(x_2)} - x_1^{f(x_1)}\right) \quad \textbf{(EQ 27)}$$

In Equation 27, M_{ic} has been replaced with M_{ia}, the coarse particle tumbling mill grinding work index.

In AG/SAG-based circuits, the need for W_s appears to be unnecessary, as primary crusher products often have a very similar gradient to typical ball mill cyclone overflows (see Figure 12). A similar situation appears to apply with HPGR product size distributions, as illustrated in Figure 13.

Weakening of HPGR Products

Laboratory experiments have been reported by various researchers in which the Bond ball work index of HPGR products is less than that of the feed (Stephenson 1997; Oestreicher and Spollen 2006; Shi et al. 2006). The amount of this reduction appears to vary with both material type and the pressing force used. Observed reductions in the Bond ball work index have typically been in the range of 0% to 10%. In the approach described in this chapter, no explicit allowance has been made for such weakening. However, if HPGR products are available that can be used to conduct Bond ball work index tests, then M_{ib} values obtained from such tests can be used in Equation 20. Note that these tests must be performed using a feed size distribution that is similar to that produced from preparing material that has not been previously treated in an HPGR (i.e., HPGR feed). The reason for this is that HPGR products tend to be relatively fine compared to conventionally crushed material. If the HPGR products are therefore used as is in a Bond test, their relatively fine distribution introduces a bias in the results. Alternatively, the M_{ib} values from Bond ball mill work index tests on HPGR feed material can be reduced by an amount that the user thinks is appropriate. Until more data become available from full-scale HPGR/ball mill circuits, it is suggested that, in the absence of Bond ball mill work index data on HPGR products, the M_{ib} results from HPGR feed material are reduced by no more than 5% to allow for the effects of microcracking.

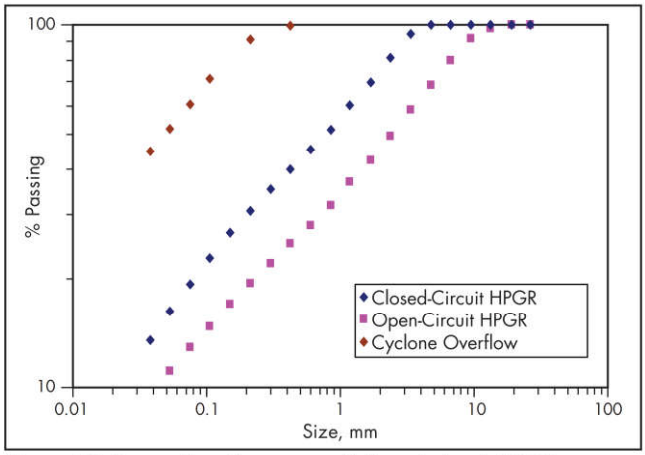

Figure 13 Examples of open- and closed-circuit HPGR distributions compared with a typical ball mill cyclone overflow distribution

Equation Accuracy

Total Specific Energy

In terms of predicting total comminution circuit specific energy, benchmarking has been conducted using data from 72 different concentrators covering more than 110 different ore types. Nine different types of circuits are covered. The results are shown in Figure 14 (Morrell 2011b). Examination of the statistics associated with the data in the figure indicates that the standard deviation of the differences between the observed and predicted values is 6.5% with an overall mean of differences of 0.2%.

AG/SAG Mills

For AG/SAG mills, benchmarking has been conducted using data from 64 different concentrators covering more than 100 different ore types (Morrell 2011a); results are shown in Figure 15. Ball mill data are shown in Figure 16. Examination of the statistics associated with the data in these figures indicates that the standard deviation of the differences between the observed and predicted values is 8.6% and 8.9%, respectively. Associated overall means of the differences are 0.6% and 0.4%, respectively.

Conventional Crushers

The crushing specific energy equations have been benchmarked using 12 different crushing circuits (25 data sets), including primary, secondary, tertiary, and pebble crushers in AG/SAG circuits (Morrell 2010). Observed versus predicted specific energies are given in Figure 17. The observed specific energies were calculated from the crusher throughput, and the net power draw of the crusher as defined by

$$\text{net power} = \text{motor input power} - \text{no-load power} \quad \textbf{(EQ 28)}$$

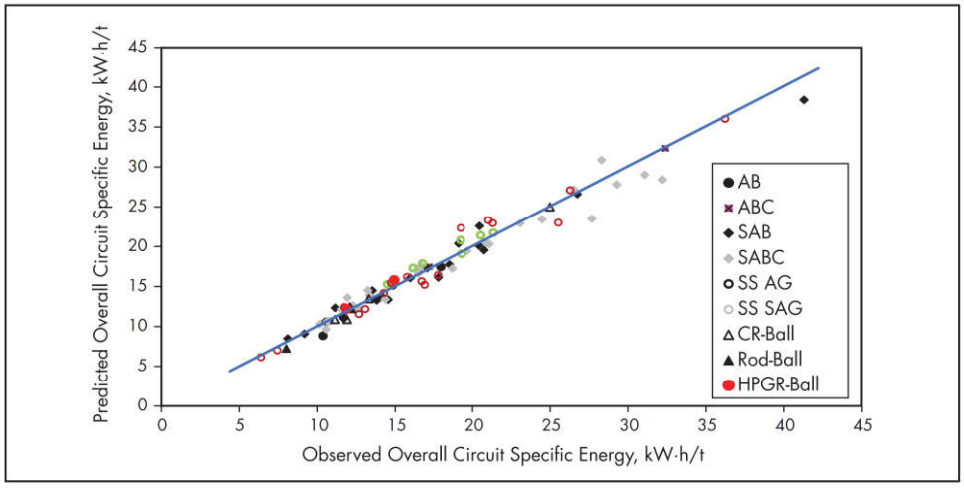

Source: Morrell 2011b

Figure 14 Predicted versus observed overall circuit specific energy

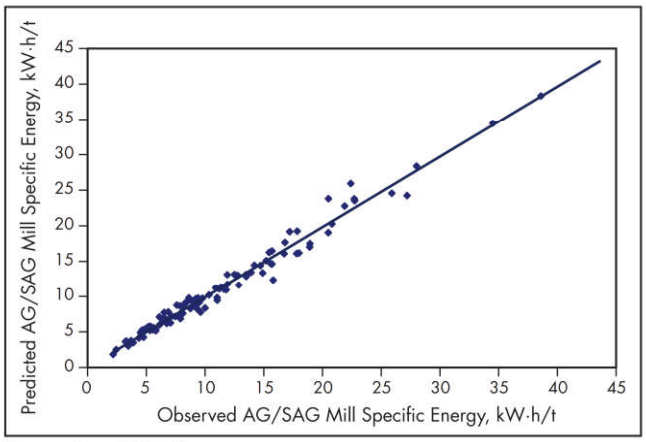

Source: Morrell 2011b

Figure 15 Predicted versus observed AG/SAG mill specific energy

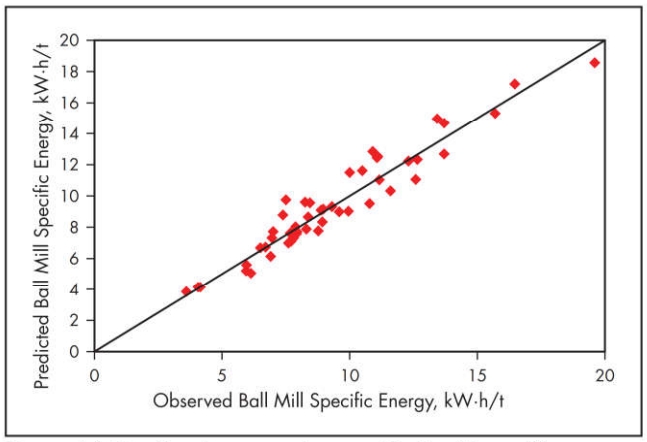

Figure 16 Predicted versus observed ball mill specific energy

No-load power tends to be relatively high in conventional crushers, and hence net power is significantly lower than the motor input power. From examination of the 25 crusher data sets, the motor input power was found to be, on average, 20% higher than the net power.

Examination of the statistics associated with the data in Figure 17 indicates that the standard deviation of the differences between the observed and predicted values is 18.1% with an overall mean of differences of 1.0%.

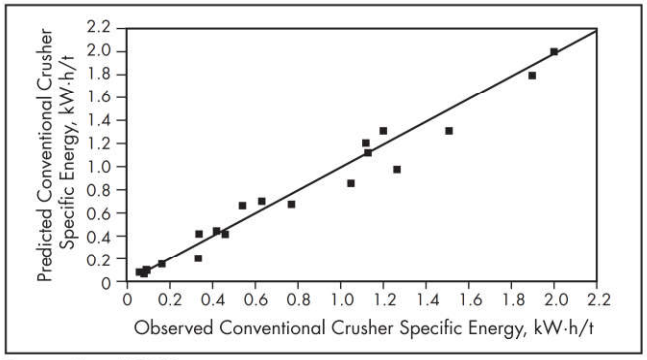

Source: Morrell 2010

Figure 17 Predicted versus observed conventional crusher specific energy

High-Pressure Grinding Rolls

The crushing specific energy equations have been benchmarked using 19 different circuits (36 data sets) including laboratory-, pilot-, and industrial-scale equipment (Morrell 2010). Observed versus predicted specific energies are given in Figure 18. The data relate to HPGRs operating with specific grinding forces typically in the range of 2.5 to 3.5 N/mm^2. The observed specific energies relate to power delivered by the roll drive shafts. Motor input power for full-scale machines is expected to be 8%–10% higher.

Examination of the statistics associated with the data in Figure 18 indicates that the standard deviation of the differences between the observed and predicted values is 8.5% with an overall mean of differences of 1.6%.

At the time of writing, more than 42,000 SMC Tests have been conducted covering more than 1,500 deposits.

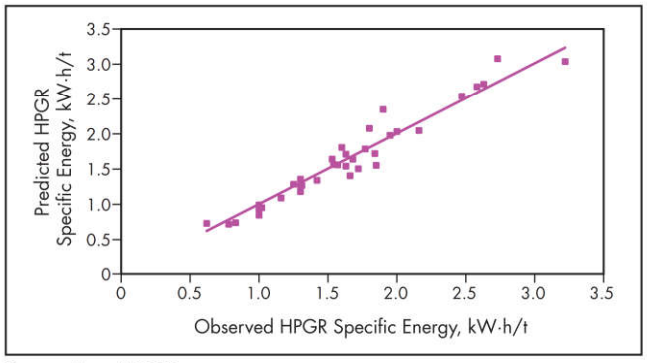

Source: Morrell 2010

Figure 18 Predicted versus observed HPGR specific energy

Worked Examples

An SMC Test and Bond ball work index test were carried out on a representative ore sample. The following results were obtained from the laboratory.

SMC Test:

- M_{ia} = 19.4 kW·h/t
- M_{ic} = 7.2 kW·h/t
- M_{ih} = 13.9 kW·h/t

Bond ball work index test:

- P_1 = 150 µm
- F_{80} = 2,250 µm
- P_{80} = 106 µm
- Gbp = 1.49 net grams of screen undersize per mill revolution
- W_{iB} = 15.15 kW·h/t
- M_{ib} = 18.8 kW·h/t (from Equation 15)

Three circuits are to be evaluated:

1. SABC
2. HPGR/ball mill
3. Conventional crushing/ball mill

The overall objective of the worked examples is to estimate the specific grinding energy to reduce a primary crusher product that has a specified P_{80} of 100 mm to a final product P_{80} that has been specified as 106 µm.

SABC Circuit

Coarse particle tumbling mill specific energy:

$$W_a = 0.95 \times 19.4 \times 4 \times \left(750^{-\left(\frac{0.295+750}{1{,}000{,}000}\right)} - 100{,}000^{-\left(\frac{0.295+100{,}000}{1{,}000{,}000}\right)}\right)$$
$$= 9.6\ \text{kW·h/t}$$

Fine particle tumbling mill specific energy:

$$W_b = 18.8 \times 4 \times \left(106^{-\left(\frac{0.295+106}{1{,}000{,}000}\right)} - 750^{-\left(\frac{0.295+750}{1{,}000{,}000}\right)}\right)$$
$$= 8.4\ \text{kW·h/t}$$

Pebble crusher specific energy: In this circuit, it is assumed that the pebble crusher feed P_{80} is 52.5 mm. As a rule of thumb, this value can be estimated by assuming that it is 0.75 of the nominal pebble port aperture (in this case, the pebble port aperture is assumed to be 70 mm). The pebble crusher is set to give a product P_{80} of 12 mm. The pebble crusher feed rate is expected to be 25% of new feed tons per hour.

$$W_c = 1.19 \times 7.2 \times 4 \times \left(12{,}000^{-\left(\frac{0.295+12{,}000}{1{,}000{,}000}\right)} - 52{,}500^{-\left(\frac{0.295+52{,}500}{1{,}000{,}000}\right)}\right)$$
$$= 1.12\ \text{kW·h/t when expressed in terms of the crusher feed rate}$$
$$= 1.12 \times 0.25\ \text{kW·h/t when expressed in terms of the SABC circuit new feed rate}$$
$$= 0.3\ \text{kW·h/t of SAG mill circuit new feed}$$

Total net comminution specific energy is therefore the sum of W_a, W_b, and W_c:

$$W_T = 9.6 + 8.4 + 0.3\ \text{kW·h/t}$$
$$= 18.3\ \text{kW·h/t}$$

HPGR/Ball Milling Circuit

In this circuit, primary crusher product is assumed to be reduced to an HPGR circuit feed P_{80} of 35 mm by closed-circuit secondary crushing. The HPGR is also in closed circuit and is assumed to reduce the 35-mm feed to a circuit product P_{80} of 4 mm. This is then fed to a closed-circuit ball mill, which takes the grind down to a P_{80} of 106 µm.

Secondary crushing specific energy:

$$W_c = 1 \times 55 \times (35{,}000 \times 100{,}000)^{-0.2} \times 7.2 \times 4 \times \left(35{,}000^{-\left(\frac{0.295+35{,}000}{1{,}000{,}000}\right)} - 100{,}000^{-\left(\frac{0.295+100{,}000}{1{,}000{,}000}\right)}\right)$$
$$= 0.4\ \text{kW·h/t}$$

HPGR specific energy:

$$W_h = 1 \times 35 \times (4{,}000 \times 35{,}000)^{-0.2} \times 13.9 \times 4 \times \left(4{,}000^{-\left(\frac{0.295+4{,}000}{1{,}000{,}000}\right)} - 35{,}000^{-\left(\frac{0.295+35{,}000}{1{,}000{,}000}\right)}\right)$$
$$= 2.4\ \text{kW·h/t}$$

Coarse particle tumbling mill specific energy:

$$W_a = 1 \times 19.4 \times 4 \times \left(750^{-\left(\frac{0.295+750}{1{,}000{,}000}\right)} - 4{,}000^{-\left(\frac{0.295+100{,}000}{1{,}000{,}000}\right)}\right)$$
$$= 4.5\ \text{kW·h/t}$$

Fine particle tumbling mill specific energy:

$$W_b = 18.8 \times 4 \times \left(106^{-\left(\frac{0.295+106}{1{,}000{,}000}\right)} - 750^{-\left(\frac{0.295+750}{1{,}000{,}000}\right)}\right)$$
$$= 8.4\ \text{kW·h/t}$$

Total net comminution specific energy is therefore

$$W_T = 4.5 + 8.4 + 0.4 + 2.4\ \text{kW·h/t}$$
$$= 15.7\ \text{kW·h/t}$$

Conventional Crushing/Ball Milling Circuit

In this circuit, primary crusher product is assumed to be reduced in size to a P_{80} of 6.5 mm via a secondary/tertiary crushing circuit (closed). This is then fed to a closed-circuit ball mill, which grinds to a P_{80} of 106 µm.

Secondary/tertiary crushing specific energy:

$$W_c = 1 \times 7.2 \times 4 \times \left(6{,}500^{-\left(\frac{0.295+6{,}500}{1{,}000{,}000}\right)} - 100{,}000^{-\left(\frac{0.295+100{,}000}{1{,}000{,}000}\right)}\right)$$
$$= 1.7\ \text{kW·h/t}$$

Coarse particle tumbling mill specific energy:

$$W_a = 1 \times 19.4 \times 4 \times \left(750^{-\left(\frac{0.295+750}{1{,}000{,}000}\right)} - 6{,}500^{-\left(\frac{0.295+6{,}500}{1{,}000{,}000}\right)}\right)$$
$$= 5.5\ \text{kW·h/t}$$

Fine particle tumbling mill specific energy:

$$W_b = 18.8 \times 4 \times \left(106^{-\left(\frac{0.295+106}{1{,}000{,}000}\right)} - 750^{-\left(\frac{0.295+750}{1{,}000{,}000}\right)}\right)$$
$$= 8.4\ \text{kW·h/t}$$

Size distribution correction:

$$W_s = 0.19 \times 19.4 \times 4 \times \left(6{,}500^{-\left(\frac{0.295+6{,}500}{1{,}000{,}000}\right)} - 100{,}000^{-\left(\frac{0.295+100{,}000}{1{,}000{,}000}\right)}\right)$$
$$= 0.9\ \text{kW·h/t}$$

Total net comminution specific energy is therefore

$$W_T = 5.5 + 8.4 + 1.7 + 0.9\ \text{kW·h/t}$$
$$= 16.5\ \text{kW·h/t}$$

SAG POWER INDEX

The SAG power index (SPI) was originally developed in the 1990s (Starkey et al. 1994) and is currently owned by SGS S.A. The test uses a 12 in. × 4 in. (D × L) batch laboratory mill loaded with 15% by volume of 1-in. balls. A picture of the mill is shown in Figure 19. The mill is loaded with 2 kg of –19 mm (P_{80} = 12.7 mm) of dry sample and run until it is ground to 80% passing 1.7 mm. The time in minutes taken to reach this grind size is designated the SPI value. An additional laboratory crushing test must also be performed, which requires 10 kg of material and generates a crushing parameter (Ci), the details of which are proprietary.

Source: Amelunxen et al. 2016
Figure 19 SPI mill

Equations

The original equation in which the SPI was used is as follows (Starkey and Dobby 1996):

$$\text{SAG kW·h/t} = (2.2 + 0.1\ \text{SPI}) / T_{80}^{0.33} \quad \textbf{(EQ 29)}$$

where T_{80} is the 80% passing size of the SAG circuit product (so-called transfer size).

Equation 29 was subsequently modified to the form shown in Equation 30 (Dobby et al. 2001).

$$\text{SAG kW·h/t} = K\ (\text{SPI} \times T_{80}^{-0.5})^n\ f_{sag} \quad \textbf{(EQ 30)}$$

where

K, n = proprietary constants
f_{sag} = feed size and pebble crusher function

The f_{sag} function is proprietary. According to Dobby et al. (2001), it is a submodel that incorporates the effects of feed size and pebble crusher circulating load (PCCL) and takes the value of unity when the circuit does not have a pebble crusher and is fed with a nominal 6-in. size distribution (F_{80}). Under these conditions, Equation 30 predicts the specific energy of a so-called "reference" or "standard" circuit (Amelunxen 2003). According to Amelunxen (2003), apart from the effects of feed size and PCCL, it also incorporates "some or all of the effects of…. differences in ball charges (or fully autogenous grinding), extremely fine grinding, low aspect-ratio mills, and open-circuit grinding. Grinding circuit audits performed on industrial-sized circuits are required for calibrating the submodel for the target circuit. There are sufficient data in the MinnovEX database to model fine feed or pebble crushing conditions without necessarily collecting plant data; however, when other conditions (such as fine grinding, low-aspect ratio mills, or open circuit SAG mills) are investigated it might be wise to first perform some calibration work before attempting to estimate the value of f_{sag}."

The f_{sag} submodel includes at least the feed size and PCCL (Dobby et al. 2001). In greenfield/brownfield design situations, these have to be predicted and hence require further submodels. Consequently, to predict the feed size distribution, Dobby et al. developed the following approach. They assumed that the feed size distribution followed a Rosin–Rammler function, and by predicting the F_{80} and F_{50} from the following equations, the entire distribution could be generated:

$$F_{80} = Ci^f SPI^g CSS^h \quad \textbf{(EQ 31)}$$

$$F_{50} = Ci^i SPI^j CSS^k \quad \textbf{(EQ 32)}$$

where Ci is the crushing parameter from laboratory crushing a sample of circuit feed, and CSS is the closed side setting of the primary crusher. The feed size distribution was then divided into three parts (designated "streams") with percentages θ_1, θ_2, θ_3. A fourth stream (θ_4) was also used and is associated with the pebble crusher circuit.

The PCCL was then estimated using the following equation:

$$PCCL = a(\theta_2 + b\theta_3/SPI^c)^d\ SPI^e \quad \textbf{(EQ 33)}$$

Equation 30 also incorporates a transfer size (T_{80}), and in greenfield/brownfield situations this also needs to be predicted. A T_{80} submodel is therefore also required and was configured using the following equations:

$$T_{80} = T_{80}(A)\ \theta_1 + T_{80}(B)\ (PCCL \times \theta_4) + T_{80}(C)\ (\theta_2 - PCCL \times \theta_4) + T_{80}(D)\ \theta_3 \quad \textbf{(EQ 34)}$$

$$T_{80}(A) = a_1\ D_1\ SPI^{b1}\ SF_A \quad \textbf{(EQ 35)}$$

$$T_{80}(B) = a_2\ D_2 SPI^{b2}\ SF_B \quad \textbf{(EQ 36)}$$

$$T_{80}(C) = a_3\ SPI^{b3} SF_C \quad \textbf{(EQ 37)}$$

$$T_{80}(D) = a_4\ P_{64}^{b4}\ SF_D \quad \textbf{(EQ 38)}$$

where

a, b, c, d, e, f, g, h, i, j, k, a_1, a_2, a_3, a_4, b_1, b_2, b_3, b_4, SF_A, SF_B, SF_C, SF_D = fitted empirical factors
D_1 and D_2 = 80% of θ_1,θ_2, respectively
SF = factors describing the effect of ball load

Including the K and n factors in Equation 30, this gives a minimum requirement of 25 empirical factors that need to be determined before Equation 30 can be used for greenfield/brownfield prediction purposes.

Validation

Kosick and Bennett (1999) reported the fitting of the empirical factors K and n in Equation 30 to data from 13 different plants that had been collected to date (see Figure 20). According to Dobby et al. (2001), further data were added to give a total of 26 plants that were used to fit the f_{sag} and T_{80} submodels in Equation 30.

From data in Starkey and Dobby (1996) and Kosick and Bennett (1999), Amelunxen et al. (2014) were able to estimate the K and n values in Equation 30 and obtained values of 5.9 and 0.55, respectively. They then used these parameters to compare the observed AG/SAG mill specific energies from 58 data sets from 14 different plants with the predicted values of the standard circuit using Equation 30. The resultant observed and predicted specific energies are reproduced in Figure 21. Additional data from Starkey and Dobby (1996) are also included, bringing the total number of data sets to 63. The obvious considerable scatter in Figure 21 results from the differences between the circuits from which the data were drawn and the standard circuit. To correct for these differences the appropriate f_{sag} values are required. Amelunxen et al. (2014) provide guidance as to what these values should be for SAG circuits with pebble crushing (f_{sag} = 0.85), AG circuits with

pebble crushing (f_{sag} = 0.62), and finer feed (i.e., F_{80} <75 mm) (f_{sag} = 0.9). When these values are applied to the standard circuit predictions, Figure 22 results. Note that the "unknown" data set is not included as the feed size or circuit configuration of these circuits is not known and hence appropriate f_{sag} values cannot be assigned to them. Scatter is reduced significantly, though there is a problem with the Holt–McDermott data, a problem that Starkey and Dobby (1996) also noted and stated needed further investigation.

Examination of the statistics associated with the data in Figure 22 indicates that the standard deviation of the differences between the observed and predicted values is 18.9% with a mean of the differences of 0.3%. If the Holt–McDermott data are not included, the results are 17.3% with a mean difference of 2.3%. However, the predicted data in Figure 22 were generated from equations that used the observed T_{80}, not modeled ones, which would be the case in greenfield/brownfield situations and would increase the scatter in Figure 22 and hence the degree of uncertainty in the predictions. As Amelunxen

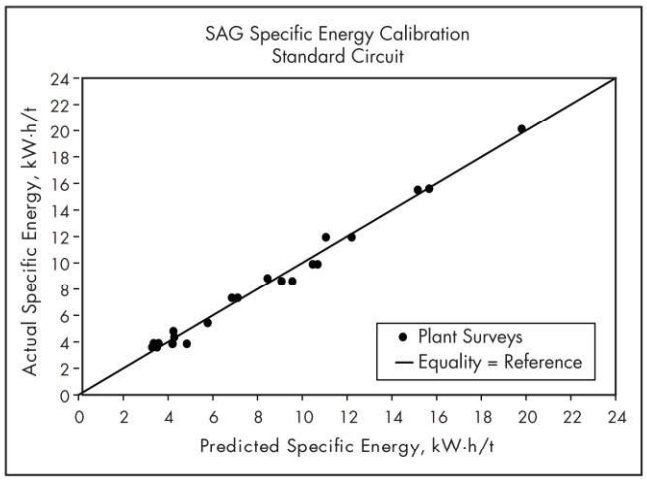

Source: Kosick and Bennett 1999

Figure 20 Calibration scatterplot

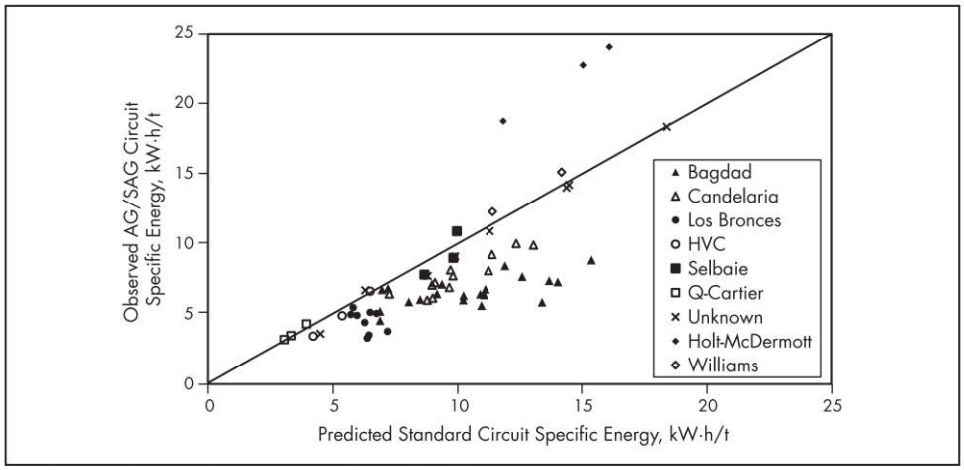

Data from Amelunxen et al. 2014 and Starkey and Dobby 1996

Figure 21 Observed AG/SAG circuit specific energy versus predicted standard circuit specific energy using the SPI

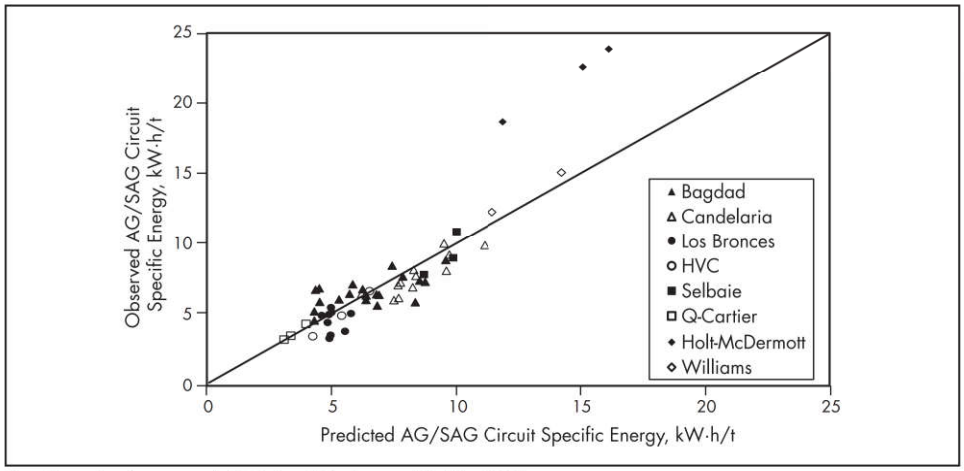

Data from Amelunxen et al. 2014 and Starkey and Dobby 1996

Figure 22 Observed versus predicted AG/SAG circuit specific energy using the SPI

et al. (2014) state, "One of the limitations of the (SPI) scale-up methodology ... is that the transfer size must be known in order to estimate the specific energy required for a given SAG mill circuit," a limitation that applies to all methodologies requiring knowledge of what the transfer will be.

At the time of writing, the website of SGS, which owns the test, states that to date the organization has performed more than 25,000 SPI Tests.

SAGDesign

The SAGDesign test was originally developed by Starkey et al. (2006) and is currently owned by Starkey and Associates Inc. The test is effectively a derivative of the SPI Test and, according to Starkey et al. (2006), during its development, "Initial work was done using SPI Test results for comparative examples." The test uses a batch mill with dimensions (D × L) 488 × 163 mm. The mill is charged with 11% by volume of a mixture of 1.5-in. and 2-in. steel balls. A minimum of 15 kg of ore is required, crushed to a P_{80} of 19 mm. Sufficient ore is added to the mill to obtain a filling of 26% by volume. The test is conducted dry and the mill is run until the charge is ground to 80% passing 1.7 mm.

Equations

The number of mill revolutions required until the charge is ground to 80% passing 1.7 mm is put into the following equation:

$$\text{SAG kW·h/t} = \text{revolutions} \times \frac{(16{,}000 + g)}{447.3g} \qquad \textbf{(EQ 39)}$$

where

SAG kW·h/t = specific energy at pinion of a SAG mill grinding from an F_{80} of 152 mm to a P_{80} of 1.7 mm

g = mass of ore added to the mill

The ground product of the mill is used as feed for a Bond ball work index test. As the size distribution is not the same as that for a conventional Bond ball work index test (should be stage-crushed to minus 3.35 mm), the resultant ball mill work index is not the same as that from a conventional Bond test (Starkey el al. 2006).

To predict the total specific energy of a single-stage SAG mill circuit or a SAG-ball mill circuit with an F_{80} of 152 mm, the kilowatt-hours per ton from Equation 39 is added to the specific energy to grind from 1.7 mm to the final grind of the circuit, which is calculated using Bond's equation following all of Bond's original recommendations for the application of his EFs. How predictions of total energy are adjusted to account for SAG circuits with F_{80} values other than 152 mm or for the inclusion/exclusion of pebble crushers is unclear.

According to Starkey and Larbi (2012), the SAG circuit specific energy is determined by first choosing a T_{80} value. In cases where this differs from 1.7 mm, the SAG kW·h/t in Equation 39 is modified by determining "values [which] are added or deducted from this basic number by calculation, using the BWI [W_{iB}] to calculate the adjustment."

For the ball mill circuit, Starkey and Larbi (2012) state that "the balance of the required power is provided by the ball mill. Here, correction factors are applied when needed."

Validation

At the time of writing, according to the SAGDesign website, more than 900 tests have been performed and benchmarking has been done using six circuits (Starkey and Larbi 2012). Four are single-stage SAG mills, of which one is a pilot mill and two are SAG–ball circuits. Observed versus predicted specific energies from these are shown in Figure 23. Benchmarking data are insufficient to provide meaningful accuracy statistics.

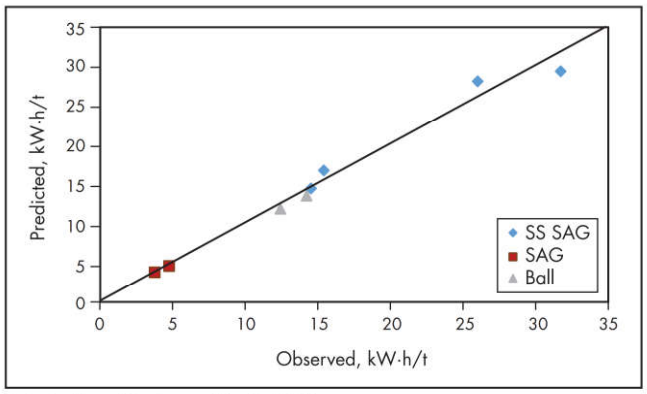

Adapted from Starkey and Larbi 2012

Figure 23 Predicted versus observed specific energy using SAGDesign approach

MACPHERSON AUTOGENOUS GRINDABILITY TEST

The MacPherson autogenous grindability test was originally developed by MacPherson in the 1970s (MacPherson and Turner 1978) and is currently owned by SGS S.A. It is a continuous test performed in an air-swept 18-in. semiautogenous mill, with an 8% ball charge and closed with a 1.2-mm screen. The test requires sufficient feed ore for the mill to reach steady state with a 28% total charge volume. This state can normally be achieved with less than 100 kg, but typically a 175-kg sample is required to allow for soft and/or dense ores. At test completion, all the products are submitted for particle size analysis, and the mill charge is dumped and observed. The charge is submitted to a particle size analysis, and size-by-size specific gravity (sg) determinations. This allows the evaluation of any coarse material build-up, or if any heavier component is present in the mill. The products from the mill at the end of the test are collected and weighed and sized.

Equations

The feed size and product size are determined, and from the measured power draw of the mill and feed rate, a Bond operating work index is determined. This result is called the autogenous work index (AWI). According to Mosher and Bigg (2001), a correction is required when harder ores are treated due to "the shortfall of high energy events in the ... mill." According to MacPherson and Turner (1978), in design situations the AWI is referenced against existing autogenous mills whose ores have also been tested using this approach and hence "the requirements of a full scale autogenous plant to treat the new ore can readily be established." No details are published as to exactly how this is done.

Validation

No published sources supply any benchmarking data that show how accurate the test is in predicting full-scale mill performance. However, according to SGS, about 750 tests have been performed on about 275 deposits.

ADVANCED MEDIA COMPETENCY TEST

The advanced media competency test (AMCT) was developed by Orway Mineral Consultants (OMC) and is a development of the Allis-Chalmers autogenous rock media competency test. The test uses a 6 ft × 1 ft batch mill and is charged with a total of 50 rocks divided equally into five size fractions in the range of 100 to 165 mm. The mill is rotated for 500 revolutions at a speed of 75% of critical, and the charge is dumped and size analyzed. The surviving rocks are sieved into five size fractions in the range of 19 to 100 mm and each size fraction is submitted to breakage in a Bond crushing work index machine. Feed samples are also subjected to the full range of Bond tests plus unconfined compressive strength (UCS) tests. Typically, 300 kg of PQ (85 mm) core is required; 180 kg is used for the tumbling test and the remainder is used for the associated Bond and UCS tests.

Although OMC originally developed the AMCT, it subsequently discontinued its use in mill selection and design due to the test's requirement for large sample masses of large-diameter drill cores (Scinto et al. 2015). OMC's approach now relies on SMC Test and drop weight test results.

OMC POWER-BASED APPROACH

OMC uses the results from the Bond ball work index, the SMC Test, and the drop weight test in a power-based methodology described by Scinto et al. (2015).

Equations

OMC's approach is similar to that developed by Morrell (2011a) in which one equation is used to estimate the total circuit specific energy and a second equation is used to predict the AG/SAG circuit specific energy. The ball mill circuit specific energy is the difference between the two values (Scinto et al. 2015).

The total energy equation developed by OMC is as follows:

$$E_{TOT} = 10 \cdot BWi \cdot [(75^{-0.5} - 150{,}000^{-0.5}) \times f_{sag} - (F_{80}^{-0.5} - 150{,}000^{-0.5}) - (75^{-0.5} - P_{80}^{-0.5})] \quad \textbf{(EQ 40)}$$

where

E_{TOT} = total grinding specific energy, kW·h/t
BWi = Bond ball mill work index, kW·h/t
f_{sag} = efficiency factor
F_{80} = feed size, 80% passing, µm
P_{80} = product size, 80% passing, µm

The details of how f_{sag} is determined are proprietary but are related to the parameters A,b and t_{10}, which are derived from SMC Test / drop weight test results.

The AG/SAG mill circuit specific energy uses the equation developed by Morrell (2011a) with the constants being fitted to OMC's database:

$$E_{SAG} = a(A \times b)^b \cdot F_{80}^c \cdot (1+d(1-e^{-gB}))^{-1} \cdot Sp^h \cdot f(Ar) \cdot f(K) \quad \textbf{(EQ 41)}$$

where

E_{SAG} = specific energy at the pinion, kW·h/t
a, b, c, d, e, g, h = empirical constants
A×b = appearance function

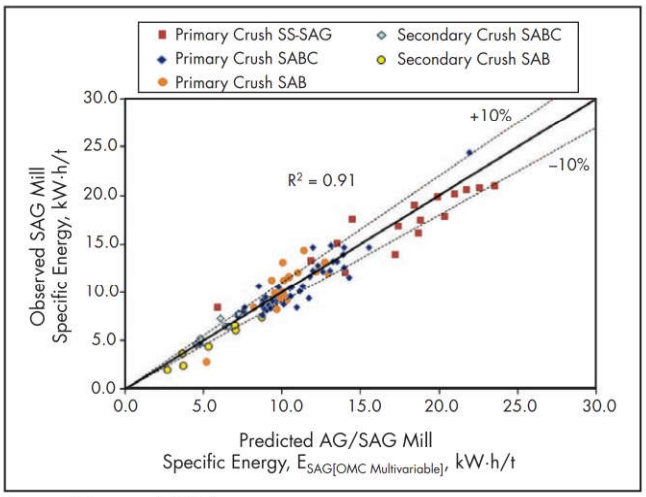

Source: Scinto et al. 2015

Figure 24 Observed versus predicted AG/SAG mill specific energy using OMC approach

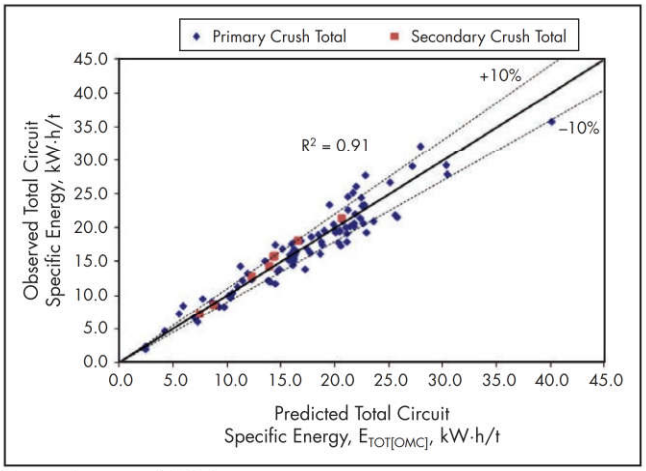

Source: Scinto et al. 2015

Figure 25 Observed versus predicted total circuit specific energy using OMC approach

F_{80} = 80% passing size of the feed
B = volume of balls, %
Sp = mill speed, % critical
f(Ar) = function of mill aspect ratio
f(K) = function for pebble crusher in circuit

Validation

OMC has benchmarked its approach using more than 100 sets of data from operating plants. The results from this benchmarking are given in Figures 24 and 25. According to Scinto et al. (2015), the average absolute error of the differences between the observed and predicted AG/SAG mill specific energies is 8.7%, and for total specific energy the associated value is 8.2%. These values are approximately equivalent to standard deviations of 11.2% and 10.4%, respectively, assuming that the mean overall difference between observed and predicted values is approximately zero.

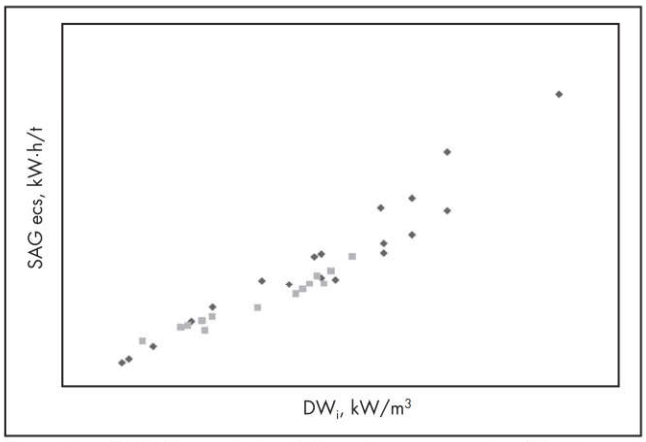

Source: Lane 2010, by permission of Gecamin, www.gecaminpublications.com

Figure 26 Correlation between the SMC Test parameter, DW$_i$, and SAG circuit specific energy

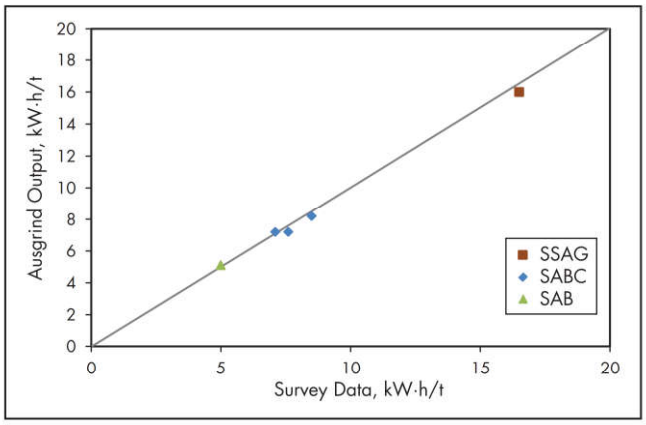

Adapted from Lane et al. 2013

Figure 27 Observed versus predicted SAG mill circuit specific energy using Ausgrind

AUSENCO POWER-BASED APPROACH

Ausenco's approach, called Ausgrind, uses the results from Bond crushing, rod, and ball work indices in conjunction with SMC Tests and is described by Lane et al. (2013).

Equations

As with OMC, Ausenco's general approach follows that developed by Morrell in which one equation is used to estimate the total circuit specific energy and a second equation is used to predict the AG/SAG circuit specific energy, the ball mill specific energy being the difference between the two. Also in line with OMC, Ausenco uses Bond equations combined with an f_{sag} correction to estimate total specific energy, the f_{sag} correction being a function of the SMC Test parameter, DW_i (Lane et al. 2013). Ausenco's total specific energy equation is as follows:

$$\begin{aligned}\text{total } E_{cs} = &(\text{Bond } E_{cs} \text{ to } 150\ \mu\text{m}) \\ &\times (f_{sag} - F_{80} \text{ effect}) \\ &\pm (\text{Bond } E_{cs} \text{ to final } P_{80})\end{aligned} \quad \textbf{(EQ 42)}$$

where E_{cs} is specific energy. In the case of Equation 42, the Bond E_{cs} value is determined following Bond's approach for a crushing/rod/ball mill circuit, though without any of the EFs applied.

For the AG/SAG circuit, Ausenco initially estimates a so-called base case circuit specific energy using a correlation with the SMC Test parameter, DW_i, that was developed using operating plant data (Figure 26). Adjustment factors (described graphically in Lane et al. 2013) are then applied to take account of various design and operating conditions such as aspect ratio, ball load, feed size, and pebble crusher performance:

$$\text{SAG } E_{cs} = (\text{base case } E_{cs}) * \text{adjustment factors} \quad \textbf{(EQ 43)}$$

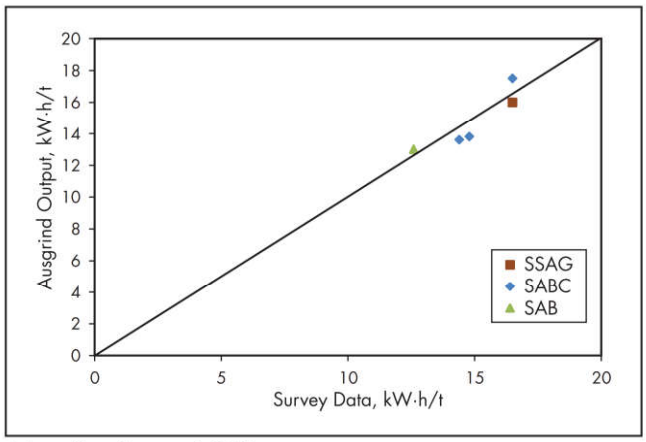

Adapted from Lane et al. 2013

Figure 28 Observed versus predicted total circuit specific energy using Ausgrind

Validation

Ausenco has published benchmarking data from three different circuits (single-stage SAG, SABC, and SAB) to illustrate the accuracy of its technique as shown in Figures 27 and 28. Benchmarking data to date is insufficient to provide meaningful accuracy statistics.

JK DROP WEIGHT TEST

The JK drop weight test uses the JK drop weight tester, which was originally developed in 1992 (Napier-Munn et al. 1996) and was precipitated by the need for a machine that could break relatively large rocks, was simple to use, was easy to maintain, and was relatively precise (i.e., had good repeatability). The device (shown in Figure 29) comprises an impact head with a hardened steel face, which can be raised to a range of heights up to ~1 m. The mass of the impact head can also be varied. The impact head is raised and a single rock is placed on a hardened steel anvil directly under the impact head. The impact head is then released and falls under the action of gravity and impacts and breaks the target particle. Through a combination of different impact head masses and heights, a very wide range of energies can be generated with which to break rocks.

The drop weight test itself typically requires about 75 kg of sample and involves breaking rocks from five different size fractions: –63+53 mm, –45+37.5 mm, –31.5+26.5 mm, –22.4+19 mm, –16+13.2 mm. If the test is conducted on drill core, it normally requires PQ (85 mm) core to provide sufficient material for the largest size fraction. Each rock size

Courtesy of JKTech Pty Ltd.

Figure 29 (A) Drop weight test in operation and (B) close-up of impact head and anvil

fraction is broken with a range of three input energies and the resultant broken particles are sized. In total, 15 sets of data are generated (5 size fractions × 3 energy levels).

The purpose of the test is to generate relationships between the energy used to break rocks and the size distribution of progeny rocks. These data are then used in simulation models of AG/SAG mills and crushers using the comminution simulator JKSimMet.

Given the relatively large sample requirement and the relatively large rock sizes also required, the test is not suitable for use with small-diameter drill core. In cases where only small-diameter drill core is available and JKSimMet modeling parameters are required, the SMC Test can be used.

Equations

Energy is related to size distribution via a data reduction process that involves the size distribution parameter, t_{10}. The t_{10} is determined from the size distribution of broken products and is defined as the percentage passing a sieve aperture 1/10 of the original particle size that was broken. The t_{10} is then determined from each of the 15 sets of size distribution data that the drop weight test generates. The relationship between the resultant t_{10} values and the associated input specific energies (E_{cs}) is fitted using the following equation (Leung 1987):

$$t_{10} = A\,(1 - e^{-b \cdot E_{cs}}) \qquad \textbf{(EQ 44)}$$

where

A and b = ore-specific parameters

E_{cs} = specific comminution energy, kW·h/t

As the impact energy is varied, the resultant t_{10} also varies, with higher impact energies producing higher values of t_{10}, which are reflected in products with finer size distributions (Figure 30).

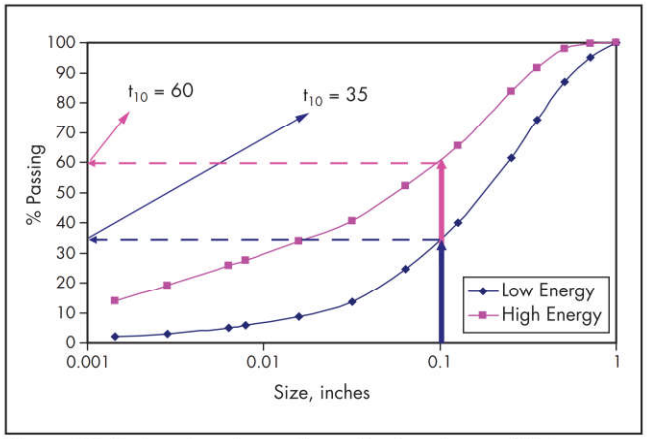

Figure 30 Estimating the t_{10} from the breakage of 1-in. particles

The t_{10} parameter and its associated use in modeling for reproducing size distributions was originally developed by Narayanan (Narayanan and Whiten 1988). Figure 30 illustrates how the t_{10} is estimated from breaking 1-in. rocks at two different energy levels. Figure 31 shows how, for a given rock size, the t_{10} varies with input energy following the shape of curve described by Equation 44. Hence, when modeling comminution machines, if the energies applied in breaking rocks can be estimated, Equation 44 can be used to predict the associated t_{10} values. As simulation models are required to predict product size distributions, this still leaves a link from the t_{10} to a size distribution to be made. This link is made using the relationships given in Figure 32. Just as the t_{10} is the percentage of broken particles that pass a sieve that is 1/10 of the original

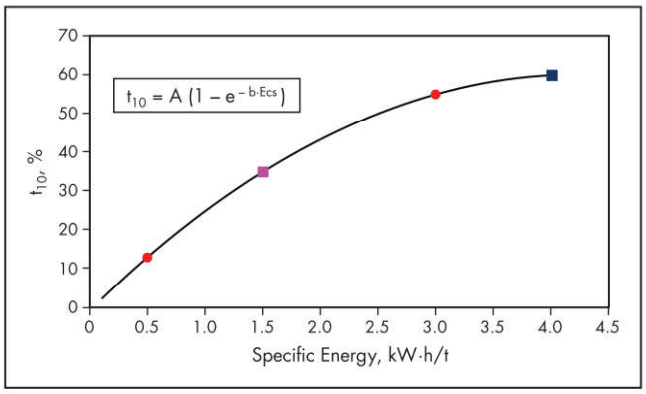

Figure 31 Variation of t_{10} with input energy for breakage of rocks in a fixed narrow size class

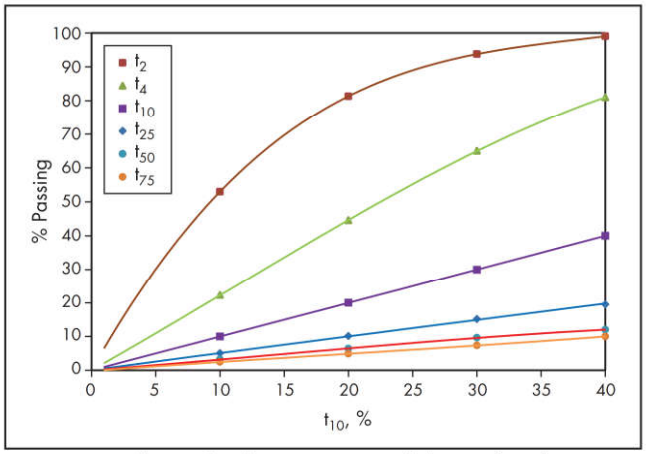

Figure 32 Relationship between t_{10} and the t_n "family" of curves

particle's size, the t_2 is the percentage of broken particles that pass a sieve that is ½ of the original particle's size, the t_{75} is the percentage of broken particles that pass a sieve that is 1/75 of the original particle's size, and so on. With reference to Figure 32, it is therefore possible to determine not only a t_{10} from a particular product size distribution but a t_2, t_4, and so on—in fact, a whole family of t_n values can be determined. Narayanan found that if the t_{10} values from breaking rocks at different energies are plotted against the associated t_2, t_4, … t_n values, the graph in Figure 32 is obtained. Narayanan found that regardless of the rock being broken, the trends shown in this figure remained largely the same; that is, the graph is a universal "map" of breakage distributions. Hence, if the t_{10} is known (e.g., from Equation 44), then the associated t_n values can be read off Figure 32. These t_n values are different points on the product size distribution curve that can thus be fully reproduced. Figure 32 and its companion Equation 44 have become central to the JK comminution modeling approach.

Whereas the drop weight test is used for simulation modeling purposes, the parameter A*b is often used in a qualitative way to indicate rock hardness. High values of A*b indicate a rock that is easy to break, while low values indicate the opposite so they work in a different manner to other rock hardness indicators. The relationship of A*b to hardness is also not linear. As a result, in terms of simulation, the difference in the predicted specific energy of a SAG mill treating an ore with an A*b of 30 and an A*b of 40 would be about 15%. However, there is only a 5% difference in the predicted specific energy when comparing ores with A*b values of 300 and 400. To help users of the drop weight test to better appreciate the differences between A*b values of different ores, JKTech recently started also reporting the SCSE (Matei et al. 2015).

The SCSE is the specific energy that would be predicted using JKSimMet of a SAG mill treating ore with the given A*b. The SAG mill circuit conditions are kept constant; that is, the SCSE always relates to the same "standard" circuit. Circuit configurations, mill designs, feed sizes, ball loads, and so on that depart from this standard will result in values that are not the same as the SCSE, and in these situations a simulation must be conducted to obtain the correct associated value. The "standard" SAG mill circuit is defined as follows:

- SAG mill:
  - Inside shell diameter to length (effective grinding length) ratio of 2:1 with 15° cone angles
  - Ball charge of 15%, 125 mm in diameter
  - Total charge of 25%
  - Grate open area of 7%
  - Apertures in the grate are 100% pebble ports with a nominal aperture of 56 mm
- Trommel: Cut size of 12 mm
- Pebble crusher: Closed-side setting of 10 mm
- Feed size distribution: F_{80} from the t_a relationship given in Equation 31 (Morrell and Morrison 1996).

$$F_{80} = 71.3 - 28.4 \ln (t_a) \quad \textbf{(EQ 45)}$$

One use of the SCSE is in evaluating the repeatability of the drop weight test. This evaluation is done on a regular basis by JKTech, which sends samples to all of the laboratories that have drop weight testers and reports on the associated statistics (Matei et al. 2015). From the latest results, the standard deviation of the relative differences between laboratories was 3.8% for the full drop weight test and 4.9% for the SMC Test.

Validation

As mentioned in the previous section, the drop weight test parameters are for use in simulation modeling and therefore validation must be in associated with a particular simulation model. The so-called Julius Kruttschnitt Mineral Research Centre (JKMRC) variable rates model is arguably the most commonly used AG/SAG mill simulation model. During its development, a total of 18 AG/SAG mills were used for benchmarking purposes (Morrell and Morrison 1996). Benchmarking was done by running the model under the same feed conditions as the full-scale mill and comparing the power draw of the actual mill with that predicted by the model. The results are shown in Figure 33 with error bars representing the 95% confidence interval. The predicted product sizes were also compared with those measured on the plant and are given in Figure 34.

Analysis of the data in Figure 25 indicates that the standard deviation of the differences between observed and predicted values is 6.4% with a mean of the differences of 3.5%.

More recently, Morrell (2004a) developed a more advanced AG/SAG model than the variable rates one and it was benchmarked using 21 different mills. The model predictions were compared with plant operating data by running the simulation model until it reached the same operating load

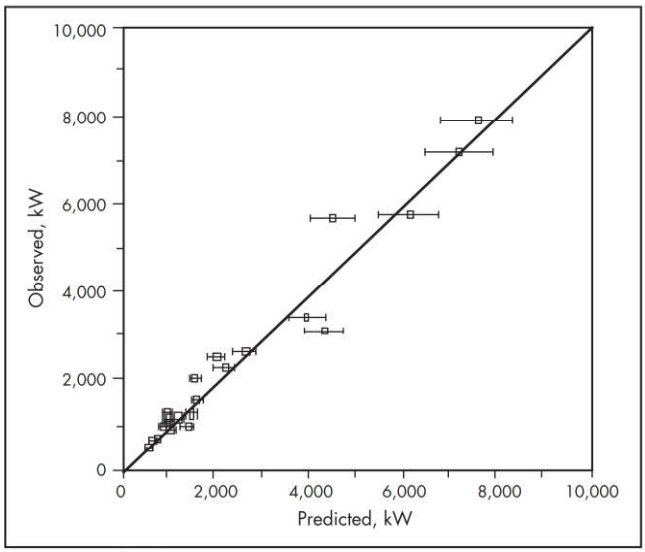

Source: Morrell and Morrison 1996

Figure 33 Observed versus predicted AG/SAG mill power draw using variable rates model

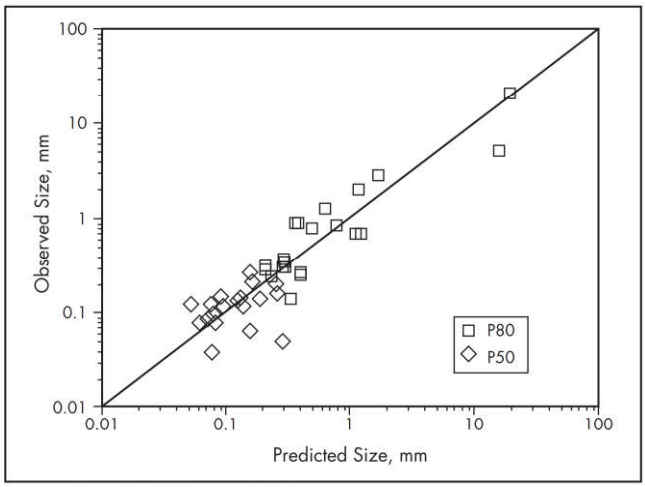

Source: Morrell and Morrison 1996

Figure 34 Observed versus predicted AG/SAG mill product size using variable rates

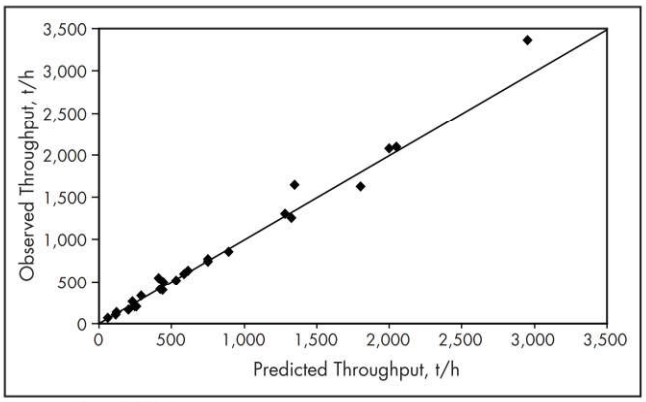

Source: Morrell 2004a

Figure 35 Observed versus predicted AG/SAG mill throughput using Morrell simulation model

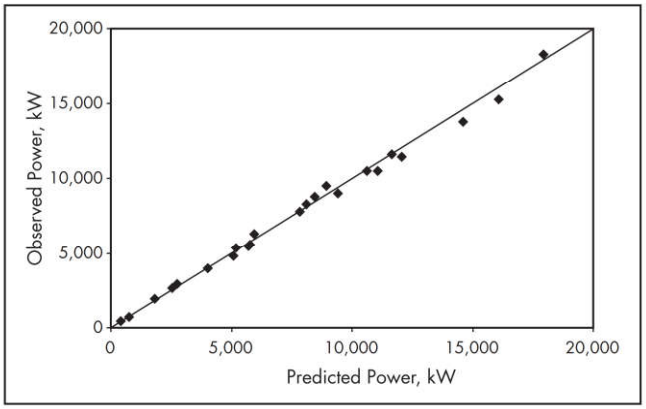

Source: Morrell 2004a

Figure 36 Observed versus predicted AG/SAG mill power draw using Morrell simulation model

that was observed on the plant. Comparisons were then made between the simulated throughput and power draw and the observed values. The results are shown in Figures 35 and 36, respectively. Comparisons of the predicted product size and the observed values were also made (Figures 37 and 38).

Analysis of the data in Figure 35 indicates that the standard deviation of differences between observed and predicted values is 11.0% with an overall mean of differences of 0.6%. For Figure 36, the associated standard deviation and mean difference are 3.8% and 0.0%, respectively.

TEST PROLIFERATION

At first sight it may appear that the proliferation of comminution characterization tests implies little consensus as to the true underlying breakage mechanisms at work in size reduction equipment. This may well be the case from a theoretical viewpoint, but from a pragmatic viewpoint there is a compelling argument that regardless of what the nature of the test is, if it can be demonstrated that it accurately predicts comminution equipment/circuit energy requirements, then it is a suitable test for the mining industry to use. Rayo (2014) illustrated this in his study of South American comminution circuits and the range of characterization techniques used in the mill selection methodology. Although this argument may help address the issue of the lack of consensus, it does not answer the question "Why are there so many tests?" To address this question, it is helpful to take a historic perspective and review when and why the different tests were developed.

The earliest tests were those developed by Bond from work begun in the 1930s and specifically targeted the most popular equipment used at that time (i.e., crushers, rod mills, and ball mills). The tests were designed to generate a single characterization value for each type of equipment (the so-called work index). In turn, the work index was used to predict the specific energy on the basis of given feed and product size distributions, the latter being described by single points (80% passing size). This methodology was termed the *power-based approach*. At this time, engineers relied on hand calculations assisted by slide rules and hand-drawn graphical techniques. Therefore, characterization tests and associated equations, of necessity, had to be simple.

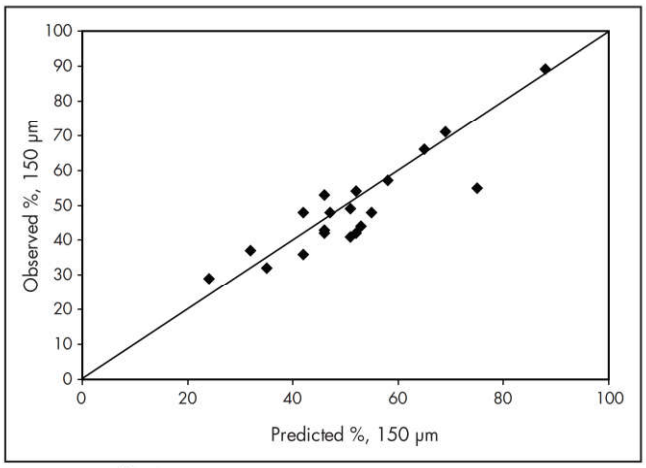

Source: Morrell 2004a

Figure 37 Observed versus predicted AG/SAG mill product size using Morrell simulation model (–150 µm)

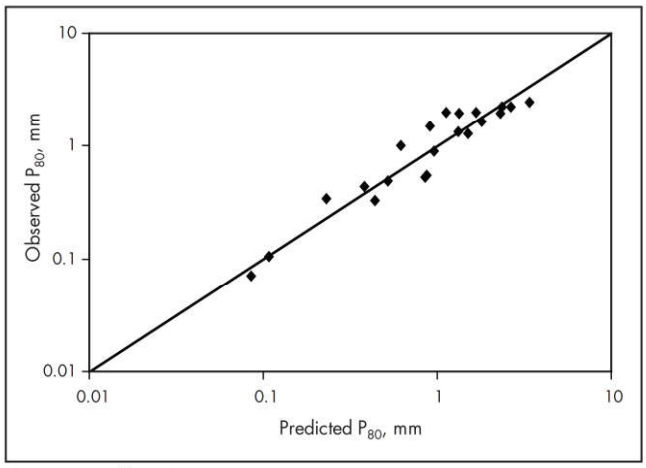

Source: Morrell 2004a

Figure 38 Observed versus predicted product size AG/SAG mill product size using Morrell simulation model (P_{80})

The rapid development of computers, particularly personal computers, in the late 1970s and the simultaneous increase in popularity of AG and SAG mills caused significant changes in minerals processing. Access to relatively powerful and inexpensive computers gave rise to the development of simulation models that attempted to mimic most aspects of the performance of comminution circuits, including power draw and predictions of mass flows and size distributions of all streams throughout the circuit—a quantum leap compared to what the power-based approach offered. Most of the simulation models used the so-called population balance equation, which in turn required ore-specific data relating to entire breakage size distributions and their relationship to breakage energy, not the single-point breakage descriptors such as the Bond tests provided. New characterization techniques were therefore required, and this drove the development of the JKMRC twin-pendulum in the early 1980s and subsequently the JK drop weight tester, which superseded it in the early 1990s. These devices were originally designed solely to provide breakage data for simulation models, which were integrated in the well-known JKSimMet comminution circuit simulator. About 75 kg of PQ core is required for the drop weight test, and therefore one of its drawbacks is that it is not suitable for small-diameter core.

The rise in popularity of AG/SAG mills initially presented designers with problems concerning equipment size selection, as at that time there were no AG/SAG breakage characterization tests similar to what was available for rod and ball mills. Initially, therefore, equipment was sized predominantly from scale-up of specific energy results from pilot tests. Pilot testing is very expensive and requires considerable amounts of ore sample (ideally, at least 400 t per ore type). Consequently, the MacPherson and autogenous rock media competency tests were developed in the late 1970s and early 1980s. They can be thought of as "mini-pilot" tests and require significantly less material than pilot tests (175 kg). Although these tests significantly reduced the amount of material required, they still had limited value for use with small-diameter drill core. At about the same time, practitioners such as Barratt and Allan (1986) attempted to combine the results from Bond's laboratory tests to predict AG/SAG circuit specific energy.

As time went on, the continued and very rapid increase in computer power gave rise to ever-sophisticated and detailed three-dimensional descriptions of ore deposits for mine planning purposes, into which process descriptions increasingly found their way—so-called geometallurgical models. Such models require significant amounts of ore characterization data so that hardness variability throughout the deposit can be adequately described. In most cases, the source of material on which hardness testing can be performed is small-diameter drill core. Given that by the early 1990s AG/SAG mills had begun to dominate circuit design, geometallurgical models increasingly required characterization tests that targeted such mills and were suitable for use with small-diameter core. To fill this need, the SPI Test was developed in the early 1990s. As with the Bond rod and ball mill tests, it uses relatively small amounts of material and grinds it in a tumbling mill to generate a single hardness parameter for use in power-based equations.

In the early 2000s and driven by the same forces, the SMC Test was developed. Unlike the SPI and Bond tests, which produce parameters that can only be used in power-based equations, the SMC Test was developed to produce parameters that can be used for both simulation modeling and power-based equations. To ensure compatibility with what had become the most popular and successful comminution simulator in the industry (JKSimMet), the SMC Test was developed for use with the JK drop weight tester.

By the mid-to-late 2000s, a sufficient number of AG/SAG mill circuits were in operation that databases being collated by some organizations such as OMC, Ausenco, and SMCC (Morrell) had become large enough to enable the development of robust semi-empirical models that reduced the variations in these databases to simple functions of hardness, equipment design, and process conditions. To varying degrees, each of these approaches uses a combination of SMC Test/drop weight test and Bond test data to characterize ore hardness.

At about the same time, an alternative but in many ways similar approach to the SPI also became available with the launch of SAGDesign. Like the SPI and Bond rod and ball mill tests, this test incorporates a tumbling mill and a size-distributed feed in contrast to the single-particle breakage

mechanisms employed by the drop weight, SMC, and Bond crushing work index tests. Industry was therefore provided with alternative approaches to predicting specific energy requirements—a prerequisite for the vital independent review stage in project development.

Although from an academic viewpoint it may seem desirable to relate different breakage mechanisms occurring in industrial comminution machines to those employed in laboratory characterization tests, in practice the validity of the test is directly related to the degree to which it correlates with industrial performance and the size and variability of the database used in the correlation, irrespective of the nature of the test. The appropriate criterion from an industry perspective, therefore, is whether the test can be successfully used to predict industrial-scale performance, and this can only be demonstrated by benchmarking using a large and varied database (e.g., Figure 14).

POWER DRAW MODELS

The simplest way to model the power draw of tumbling mills is to consider the power associated with a solid rotating body, in which case the following equation applies:

$$\text{power (P)} = 2\pi N\tau \quad \textbf{(EQ 46)}$$

where

N = rotational rate, in revolutions per unit time
τ = torque

Torque (τ) is defined as the product of force (F) and distance (s) when the force is applied to assist or retard the rotation of a body. The distance (s) is measured at right angles to the direction of force and joins the line of force to the axis of rotation of the body. An example of a simple system where a force is applied to retard rotation is shown in Figure 39. The torque in this case is given by

$$\text{torque } (\tau) = F \cdot s \quad \textbf{(EQ 47)}$$

where s is the distance between center of rotation and centroid of gravity of the charge (often referred to as the torque or lever arm distance).

Equation 47 describes the relationship between torque and power in a simple system. This relationship can be extended to tumbling mills, usually by assuming that the charge takes the shape shown in Figure 40. This shape results from the rotation of the mill shell, which "holds the charge up" in approximately the position shown. By considering the charge as a solid mass with a weight (W) and remembering that weight is a force (mass × gravitational acceleration), the torque that it applies against the rotation of the mill is given by

$$\text{torque } (\tau) = W \cdot s \quad \textbf{(EQ 48)}$$

Hence the power draw is given by

$$\text{power} = 2\pi \cdot W \cdot s \cdot N \quad \textbf{(EQ 49)}$$

where

W = charge weight
s = lever arm distance
$W \cdot s$ = torque
N = rotational rate (speed)

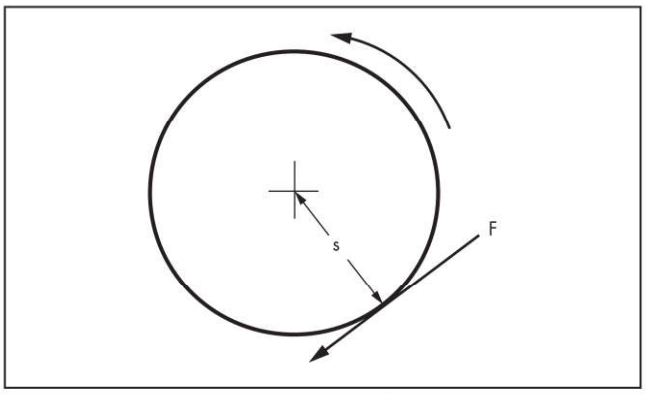

Figure 39 Example of torque as applied to a simple system

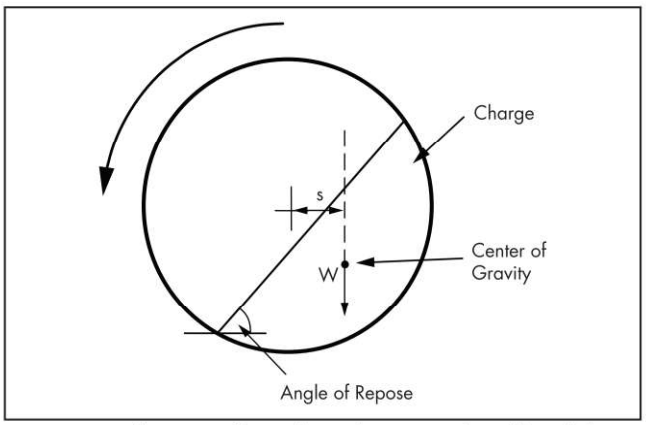

Figure 40 Schematic of grinding charge inside mill and the torque it applies

Equation 49 can be rewritten in a more general form as follows:

$$\text{power} = K\, D^n\, L\, \rho\, f(\phi)\, g(J) \quad \textbf{(EQ 50)}$$

where

K = constant for a particular design/use of mill and is different for different designs/uses (e.g., overflow ball mill, grate discharge ball mill, rod mill, autogenous mill, or semiautogenous mill)
D = mill diameter
n = the diameter exponent that in theory should be 2.5
L = mill length
ρ = charge density
$f(\phi)$ = function of mill speed (ϕ) where speed is represented as the fraction of critical
$g(J)$ = function of mill charge volume (J) where J is expressed as the fraction of mill volume occupied by the charge

Many published models in the literature can be derived using Equation 50 (Bond 1962; Hogg and Fuerstenau 1972; Harris et al. 1985; Austin 1990). Rose and Evans (1956a, 1956b) and Morrell (1993), however, are some of the few who took a different route.

Bond Model

The original form of Bond's (1961) grinding mill power equation is as follows:

$$kWb = 2.8D^{0.4}\,(3.2 - 3Vp)\,C_s\,(1 - 0.1/2^{(9-10C_s)}) \quad \textbf{(EQ 51)}$$

where

kWb = mill input kW (power at pinion) per ton of grinding balls in overflow wet grinding mills
D = interior mill diameter, ft
V_p = fraction of mill volume occupied by balls
C_s = fraction of critical speed

Equation 51 was first published in January 1961. However, in April 1962 it was revised, presumably on the basis of further operational data. Equation 51 was therefore changed to

$$kWb = 3.1D^{0.3}\,(3.2 - 3V_p)\,C_s\,(1 - 0.1/2^{(9-10C_s)}) \quad \textbf{(EQ 52)}$$

For grate discharge mills, kWb was multiplied by

$$1 + \frac{0.4 - V_{pd}}{2.5}$$

where V_{pd} is 0.029 for wet-grinding grate and low-level discharge mills. The previous term, when evaluated using V_{pd} = 0.029, gives a value of 1.1484. Converting Equation 52 into metric units and using a notation consistent with the other equations gives

$$\text{power (kW)} = 12.262\rho_b\phi LD^{2.3} \times J_B(1 - 0.937J_B)\left(1 - \frac{0.1}{2^{9-10\phi}}\right) \quad \textbf{(EQ 53)}$$

Bond's equation was meant for ball mills and therefore in Equation 53 the bulk ball density (ρ_b) is used (i.e., the contribution of the slurry fraction is not explicitly incorporated). To extend the application of the equation to SAG and AG mills, ρ_b was replaced with the bulk density of the ball and/or rock charge (ρ_c) (Morrell 1993). As with Bond's ball mill power equation, the slurry fraction was not included. The charge density was therefore defined as

$$\rho_c = (1 - E)\frac{(J_B\rho_b + J_o\rho_o)}{J_t} \quad \textbf{(EQ 54)}$$

where

E = grinding media voidage = 0.4
J_B = fractional ball filling
ρ_b = steel specific gravity = 7.8
J_o = fractional ore filling (excluding slurried ore)
ρ_o = ore specific gravity
J_t = total fractional filling = $J_B + J_o$

For ball mills, Equation 54 reduces to $\rho_c = 0.6 \times 7.8$, which is the bulk density of the balls as per Bond's original equation. Bond's grate discharge correction was also applied to SAG and AG mills.

Validation

The mill power draw database that was published by Morrell (1993) and is reproduced in Tables 2–4 was used to evaluate the Bond power draw model. Results are shown graphically in Figures 41 and 42. Statistical analysis of results shows that for ball mills, the standard deviation of the differences between observed and predicted values is 4.7% with the overall mean of differences being 2.3%. For AG/SAG mills, the associated figures are 14.7% and 13.1%, respectively. The results indicate that for ball mills the Bond model is very good, but it is quite poor for AG/SAG mills. This is perhaps not surprising, as Bond developed his model with only ball mills in mind.

Harris et al. Model

Harris et al. (1985) adopted a torque-arm approach, envisioning the mill contents as per Figure 43. Their approach led to the following equation:

$$P = \frac{\pi\rho g N L D^3 \sin^3\theta \sin\alpha}{6} \quad \textbf{(EQ 55)}$$

where

P = mill power, kW
ρ = bulk density of the charge, t/m^3
g = gravitational constant, m/s^2
N = mill speed, rps
L = mill length, m
D = mill diameter, m
θ = half-angle subtended by the charge (see Figure 43)
α = angle of repose

This equation is essentially the same as that obtained by Hogg and Fuerstenau (1972), who used a potential energy approach in their work and envisioned the contents of the mill as per Figure 44.

The term $\sin^3\theta$ in Equation 55 was approximated by Harris et al. (1985) as follows:

$$\sin^3\theta = 4L_f(1 - L_f) \quad \textbf{(EQ 56)}$$

This leads to the equation:

$$P = 1.333\pi D^3 L\rho_c N J_t(1 - J_t)g\sin\alpha \quad \textbf{(EQ 57)}$$

where

P = mill power, kW
D = mill diameter, m
L = mill length, m
ρ_c = bulk density of the charge, t/m^3
N = mill speed, rps
J_t = fraction of mill volume occupied by grinding media, measured at rest

The bulk density was calculated as follows:

$$\rho_c = \frac{(J_b\rho_b + J_o\rho_o)}{J_t}(1 - E) + E\rho_s \quad \textbf{(EQ 58)}$$

where

J_b = fractional ball filling
ρ_b = steel specific gravity = 7.85
J_o = fractional rock filling: $J_o = J_t - J_b$
ρ_o = ore specific gravity
E = grinding media voidage = 0.4
ρ_s = slurry specific gravity

To determine $\sin\alpha$, Harris et al. (1985) fitted Equation 57 to a range of manufacturer's data and obtained the following values:

Table 2 Ball mill power draw data

Discharge Mechanism	Diameter Inside Liners, m	Length (belly), m	Length (C/line), m	Length/ Diameter Ratio	Mill Speed, fraction of critical	Mill Speed, rpm	Ball Filling, %	Total Filling, %	Ore Specific Gravity	Gross Power, kW
Overflow	4.41	6.10	6.10	1.38	0.74	14.86	35	35	4.10	1,900.00
Overflow	2.30	4.20	4.20	1.83	0.82	22.87	36	36	2.70	299.00
Overflow	2.65	3.40	3.40	1.28	0.77	20.08	36	36	2.70	334.00
Overflow	2.52	3.66	3.66	1.45	0.67	17.98	35	35	2.70	265.00
Grate	1.73	2.44	2.44	1.41	0.68	22.03	35	35	2.70	97.00
Overflow	3.48	4.62	4.62	1.33	0.71	16.10	39	39	2.70	834.00
Overflow	3.54	4.88	4.88	1.38	0.76	17.20	42	42	2.70	1,029.00
Overflow	4.12	5.49	5.49	1.33	0.75	15.57	45	45	2.70	1,600.00
Overflow	4.38	7.45	7.45	1.70	0.75	15.16	30	30	2.70	2,026.00
Overflow	5.29	7.32	7.32	1.38	0.70	12.87	40	40	3.20	3,828.00
Overflow	4.80	6.10	6.10	1.27	0.69	13.32	40	40	3.00	2,498.00
Overflow	3.05	4.27	4.27	1.40	0.70	16.95	40	40	4.50	580.00
Overflow	2.60	3.70	3.70	1.42	0.69	18.10	40	40	4.50	347.00
Overflow	3.05	4.27	4.27	1.40	0.73	17.68	45	45	3.90	600.00
Overflow	3.50	4.42	4.42	1.26	0.74	16.73	35	35	2.75	820.00
Overflow	4.87	8.84	8.84	1.82	0.72	13.80	27	27	2.60	2,900.00
Overflow	4.87	8.84	8.84	1.82	0.75	14.37	30	30	2.60	3,225.00
Overflow	4.87	8.80	8.80	1.81	0.75	14.37	31	31	2.60	3,104.00
Overflow	5.33	8.54	8.54	1.60	0.72	13.23	34	34	2.60	4,100.00
Overflow	3.04	3.05	3.05	1.00	0.82	19.77	45	45	3.50	475.00
Overflow	2.29	2.74	2.74	1.20	0.83	23.11	44	44	3.50	235.00
Grate	1.70	2.70	2.70	1.59	0.81	26.27	40	40	2.70	103.00
Overflow	3.55	4.87	4.87	1.37	0.72	16.16	40	40	2.80	970.00
Overflow	3.50	4.75	4.75	1.36	0.75	16.95	42	42	2.80	921.00
Overflow	0.85	1.52	1.52	1.79	0.71	32.57	40	40	2.90	10.00
Overflow	0.85	1.52	1.52	1.79	0.71	32.57	20	20	2.90	6.80
Overflow	4.75	6.26	6.26	1.32	0.77	14.94	28	28	2.68	2,050.00
Overflow	3.85	5.90	5.90	1.53	0.77	16.60	30	30	2.80	1,300.00
Grate	2.64	3.66	3.66	1.39	0.70	18.22	43	43	2.80	420.00
Overflow	4.12	7.04	7.04	1.71	0.70	14.69	38	38	2.60	1,800.00
Overflow	4.10	5.92	5.92	1.44	0.75	15.67	34	34	3.10	1,525.00
Overflow	4.35	6.56	6.56	1.51	0.70	14.19	40	40	2.72	1,850.00
Overflow	3.48	6.33	6.33	1.82	0.75	17.00	34	34	2.70	1,150.00
Overflow	3.83	4.83	4.88	1.26	0.61	13.29	31	31	2.60	842.00
Overflow	4.68	5.64	5.64	1.21	0.72	14.08	48	48	2.80	2,300.00
Overflow	4.73	7.01	7.01	1.48	0.60	11.76	32	32	2.80	1,840.00
Overflow	5.34	8.69	8.69	1.63	0.73	13.36	28	28	3.20	3,669.00
Overflow	5.34	8.69	8.69	1.63	0.73	13.36	26	26	3.20	3,549.00
Overflow	5.34	8.69	8.69	1.63	0.73	13.36	24	24	3.20	3,385.00
Overflow	5.34	8.69	8.69	1.63	0.73	13.36	23	23	3.20	3,251.00
Overflow	3.87	6.34	6.34	1.64	0.69	14.83	27	27	4.60	1,075.00
Number	41	41	41	41	41	41	41	41	41	41
Mean	3.73	5.58	5.58	1.49	0.73	17.06	35.25	35.32	3.03	1,539.34
Standard deviation	1.23	2.15	2.15	0.21	0.05	4.73	6.79	6.80	0.55	1,223.53
Minimum	0.85	1.52	1.52	1.00	0.60	11.76	20	20	2.60	6.80
Maximum	5.34	8.84	8.84	1.83	0.83	32.57	48	48	4.60	4,100.00

Table 3 SAG mill power draw data

Discharge Mechanism	Diameter Inside Liners, m	Length (belly), m	Length (C/line), m	Length/ Diameter Ratio	Mill Speed, fraction of critical	Mill Speed, rpm	Ball Filling, %	Total Filling, %	Ore Specific Gravity	Gross Power, kW
Grate	w	3.46	3.46	0.45	0.70	10.65	11	11	2.60	1,800.00
Grate	6.50	2.42	3.02	0.37	0.75	12.44	6	21	3.64	1,228.00
Grate	4.35	4.85	4.85	1.11	0.75	15.29	12	29	2.60	1,045.00
Grate	7.05	3.45	3.45	0.49	0.72	11.47	12	33	2.65	2,239.00
Grate	7.05	3.45	3.45	0.49	0.72	11.47	12	12	2.65	1,500.00
Grate	5.30	7.95	7.95	1.50	0.71	13.04	18	30	2.80	3,284.00
Grate	4.05	4.60	4.60	1.14	0.76	15.97	8	26	2.70	688.00
Grate	4.05	4.60	4.60	1.14	0.76	15.97	7	7	2.70	440.00
Grate	4.05	4.60	4.60	1.14	0.76	15.97	6	32	2.70	687.00
Grate	4.05	4.60	4.60	1.14	0.76	15.97	6	34	2.70	706.00
Grate	6.51	2.44	2.44	0.38	0.71	11.77	3	16	4.10	972.00
Grate	1.80	0.59	0.59	0.33	0.75	23.55	6	27	2.74	14.80
Grate	9.59	4.27	5.86	0.45	0.75	10.24	14	14	2.60	5,790.00
Grate	9.59	4.27	5.86	0.45	0.75	10.24	19	31	2.60	7,900.00
Grate	9.59	4.27	5.86	0.45	0.75	10.24	17	30	2.60	7,100.00
Grate	8.39	3.26	5.00	0.39	0.80	11.69	14	18	2.68	4,000.00
Grate	4.12	5.02	5.02	1.22	0.75	15.63	22	22	2.70	1,012.00
Grate	4.12	5.02	5.02	1.22	0.75	15.63	22	33	2.70	1,225.00
Grate	4.16	4.78	4.78	1.15	0.89	18.44	10	38	2.70	1,063.00
Grate	3.90	5.10	5.10	1.31	0.78	16.75	25	34	3.35	1,175.00
Grate	5.08	6.82	6.82	1.34	0.66	12.38	12	31	2.85	2,000.00
Grate	5.05	5.99	5.99	1.19	0.77	14.49	17	21	2.68	2,035.00
Grate	5.82	5.65	5.65	0.97	0.81	14.20	13	33	2.80	2,840.00
Grate	5.80	5.65	5.65	0.97	0.81	14.20	10	27	2.80	2,600.00
Grate	3.85	5.69	5.69	1.48	0.48	10.35	12	12	2.80	424.00
Grate	7.23	3.00	3.00	0.42	0.75	11.80	11	16	2.72	1,920.00
Grate	7.09	2.74	2.74	0.39	0.75	11.91	11	21	3.10	1,900.00
Grate	6.26	2.50	2.50	0.40	0.71	12.00	5	21	2.70	1,200.00
Number	28	28	28	28	28	28	28	28	28	28
Mean	5.79	4.32	4.57	0.84	0.74	13.71	12.16	24.25	2.82	2,099.49
Standard deviation	2.01	1.52	1.55	0.41	0.07	3.03	5.67	8.52	0.34	1,946.55
Minimum	1.80	0.59	0.59	0.33	0.48	10.09	3	7	2.60	14.80
Maximum	9.59	7.95	7.95	1.50	0.89	23.55	25	38	4.10	7,900.00

Mill type	sinα
Autogenous	0.707
Overflow	0.682
Grate	0.809

The mill filling component of Equation 57 was also modified to account for mills with a relatively low filling. Therefore:

$$P = 1.33\pi D^3 L\rho_c NJ_t(1 - J_t)g \sin\alpha; \quad 0.35 < J_t < 0.5 \qquad \textbf{(EQ 58a)}$$

$$P = 1.33\pi D^3 L\rho_c NJ_t(1.05 - 1.133J_t)g \sin\alpha; \quad 0.2 < J_t < 0.35$$

Validation

The mill power draw database that was published by Morrell (1993) and is reproduced in Tables 2–4 was used to evaluate the Harris et al. power draw model. Results are shown graphically in Figures 45 and 46. Statistical analysis of results shows that for ball mills, the standard deviation of the differences between observed and predicted values is 9.7% with an overall mean of differences of 27.1%. For AG/SAG mills, the associated figures are 11.6% and 11.9%, respectively. The results indicate that for both ball and AG/SAG mills, if the inherent bias were to be corrected, it is a reasonable model.

Table 4 AG mill power draw data

Discharge Mechanism	Diameter Inside Liners, m	Length (belly), m	Length (C/line), m	Length/ Diameter Ratio	Mill Speed, fraction of critical	Mill Speed, rpm	Total Filling, %	Ore Specific Gravity	Gross Power, kW
Grate	7.10	2.43	3.47	0.34	0.72	11.43	10	3.57	703.00
Grate	7.10	2.43	3.47	0.34	0.72	11.43	12	4.60	1,009.00
Grate	6.49	2.25	2.48	0.35	0.75	12.45	27	4.00	1,240.00
Grate	6.49	2.25	2.48	0.35	0.75	12.45	19	4.00	960.00
Grate	5.11	5.18	5.18	1.00	0.73	13.63	24	4.20	1,264.00
Grate	1.80	0.59	0.59	0.33	0.75	23.55	25	2.74	12.50
Grate	9.50	4.40	6.40	0.46	0.75	10.29	31	2.90	5,490.00
Number	7	7	7	7	7	7	7	7	7
Mean	6.23	2.79	3.44	0.45	0.74	13.60	21.11	3.72	1,525.50
Standard deviation	2.35	1.53	1.90	0.25	0.01	4.51	7.78	0.69	1,799.05
Minimum	1.80	0.59	0.59	0.33	0.72	10.29	10	2.74	12.50
Maximum	9.50	5.18	6.40	1.00	0.75	23.55	31	4.60	5,490.00

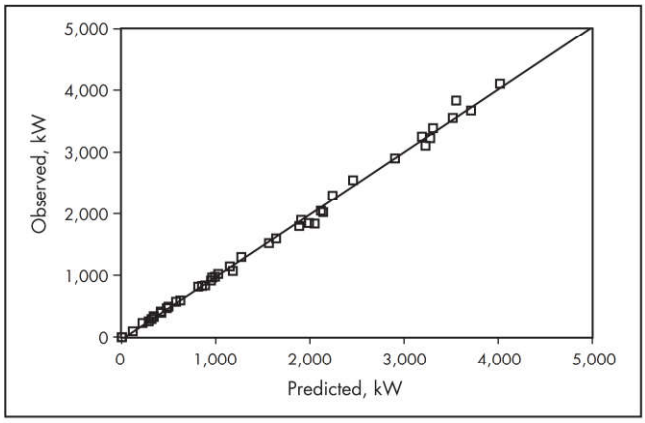

Source: Morrell 1993

Figure 41 Observed versus predicted power draw of ball mills using the Bond model

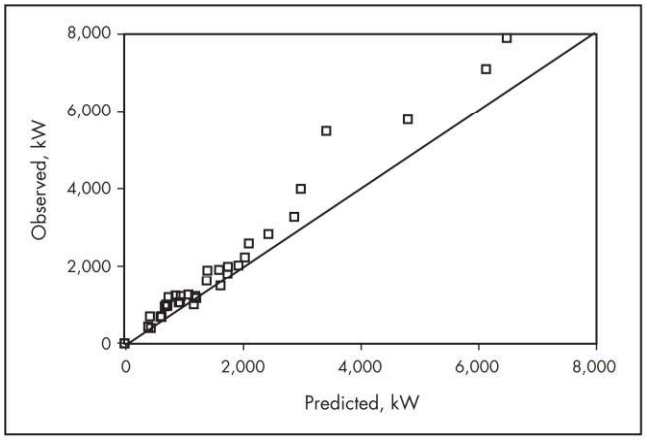

Source: Morrell 1993

Figure 42 Observed versus predicted power draw of AG/SAG mills using the Bond model

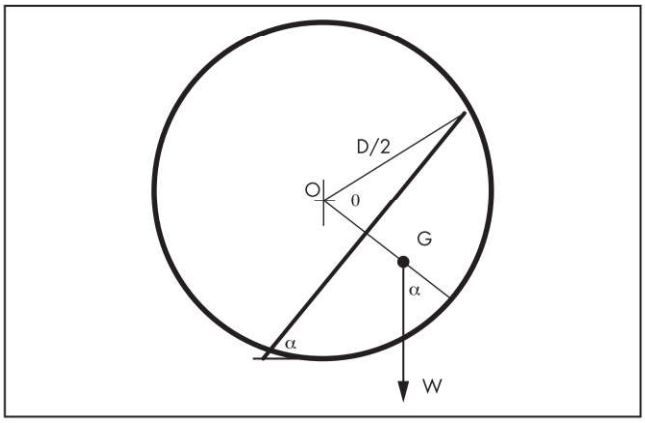

Source: Morrell 1993

Figure 43 Torque-arm treatment of power draw

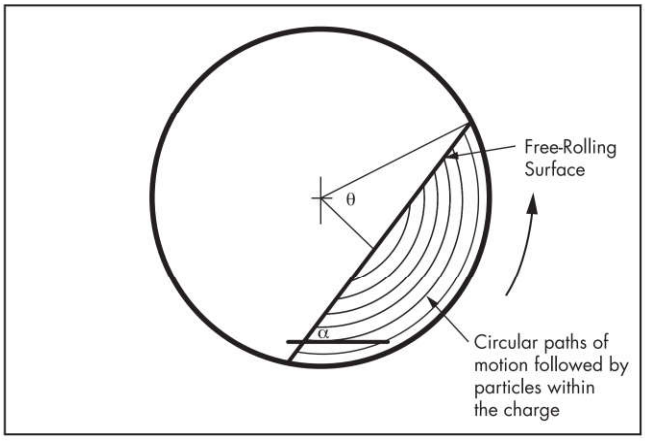

Source: Morrell 1993

Figure 44 Idealized charge motion used by Hogg and Fuerstenau (1972)

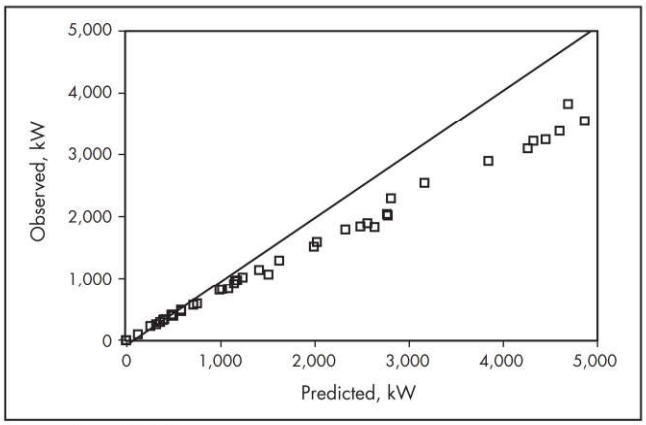

Source: Morrell 1993

Figure 45 Observed versus predicted power draw of ball mills using the Harris et al. (1985) model

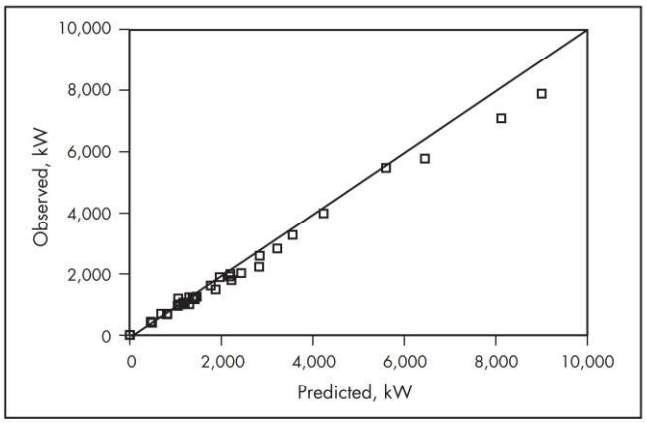

Source: Morrell 1993

Figure 46 Observed versus predicted power draw of AG/SAG mills using the Harris et al. (1985) model

Austin Model

From his literature search, Austin (1990) concluded that for semiautogenous mills there were no generally accepted mill power equations comparable to those of Bond. He therefore used elements of Hogg and Fuerstenau's (1972) and Bond's (1962) equations, plus additional modifications, to provide a model that was claimed to be suitable for SAG mills with both high and low aspect ratios. However, the inherent form of his model appears equally suitable for ball mills. His equation is written as follows:

$$M_p = 10.6D^{2.5}L(1 - 1.03J_t)[1 - E_B)\left(\frac{\rho_s}{w_c}\right)J_t + 0.6J_B\left(\rho_b - \frac{\rho_s}{w_c}\right)](\phi_c)\left(1 - \frac{0.1}{2^{9-10\phi_c}}\right)(1 + f_3) \quad \textbf{(EQ 59)}$$

where

M_p = net mill power (power at pinion), kW
D = mill internal diameter, m
L = mill length, m
J_t = fractional volume of cylindrical mill filled by total charge
E_B = porosity of total charge = 0.3

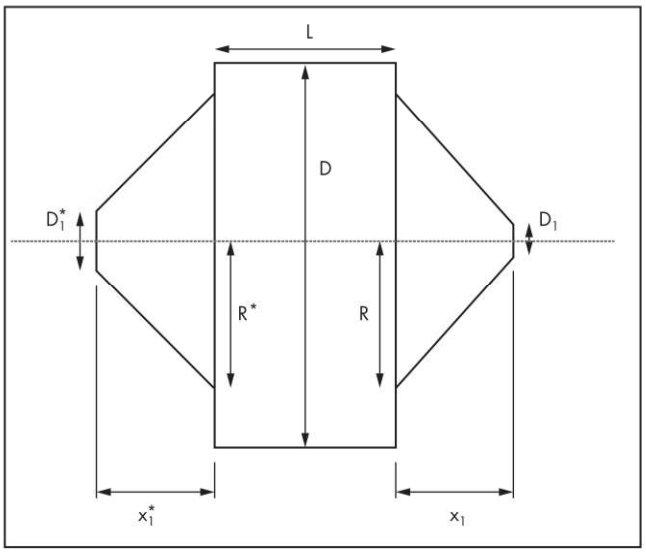

Source: Austin 1990

Figure 47 Schematic of mill with cone ends

ρ_s = mean density of rock, t/m^3
w_c = weight fraction of rock to water and rock in the mill charge ≈ 0.88
J_B = fractional volume of cylindrical mill filled by balls only
ρ_b = density of ball material, t/m^3 = 7.9 t/m^3
ϕ_c = mill rotational speed as a fraction of critical speed
f_3 = conical end correction

Austin developed an equation for predicting the power draw of the conical ends by considering the power draw of the elements shown in Figure 47 and integrating with respect to the filled length of the cone. Rewriting Austin's original correction term (f_3) on the assumption that both cone ends are identical gives

$$f_3 = \frac{2 \times 0.046}{J(1 - 1.03J)}\left\{\left(\frac{x_1/L}{1 - D_1/2R}\right)\left[\left(\frac{1.25R/D}{0.5 - J}\right)^{0.1} - \left(\frac{0.5 - J_t}{1.25R/D}\right)^4\right]\right\} \quad \textbf{(EQ 60)}$$

where

x_1 = length of the cone section, m
D_1 = trunnion diameter, m
R = maximum radius of cone section, m

Validation

The mill power draw database that was published by Morrell (1993) and is reproduced in Tables 2–4 was used to evaluate the Austin power draw model. Results are shown graphically in Figures 48 and 49. Statistical analysis of results shows that for ball mills, the standard deviation of the differences between observed and predicted values is 9.4% with an overall mean of differences of 19.2%. For AG/SAG mills, the associated figures are 13.8% and 9.9%, respectively. The results indicate that as with the Harris et al. model, there is considerable bias, both for ball and AG/SAG mills. For ball mills, Austin's model is on par with Harris et al.'s, but in the case of AG/SAG mills, it is not as good and can be considered relatively poor.

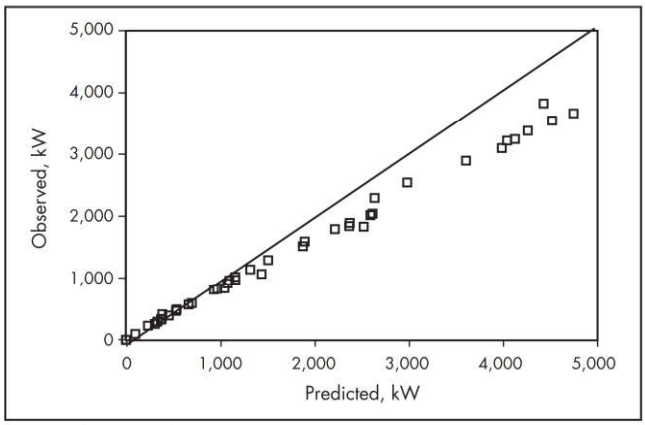

Source: Morrell 1993

Figure 48 Observed versus predicted power draw of ball mills using the Austin model

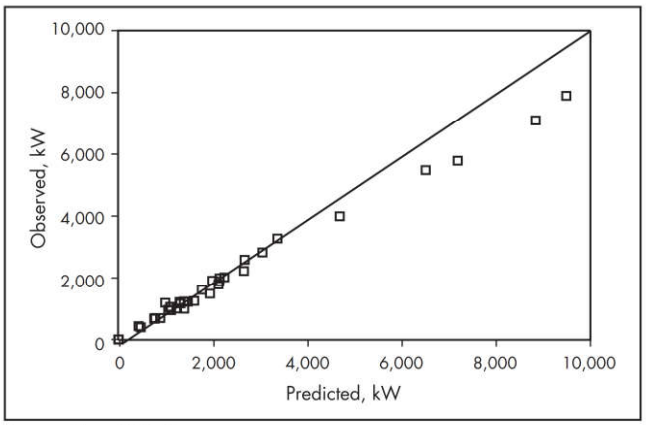

Source: Morrell 1993

Figure 49 Observed versus predicted power draw of AG/SAG mills using the Austin model

Rose and Evans Model

The contributions of the work conducted by Rose and Evans are reported in the first two papers of a trilogy written between 1954 and 1955 and published in 1956 (Rose and Evans 1956a, 1956b; Rose and Blunt 1956).

The work of these two researchers was the first, and so far remains the most thorough, investigation of most of the factors that might reasonably be expected to affect grinding mill power draw. However, the work was conducted using mills of less than 3 in. in diameter.

Dimensional analysis was used to develop the following equation:

$$\frac{P}{D^5N^3\rho} = \phi\left\{\left(\frac{h}{D}\right),\left(\frac{d}{D}\right),\left(\frac{g}{DN^2}\right),\left(\frac{b}{D}\right),\left(\frac{H}{D^6N^2\rho^2}\right),\left(\frac{\nu}{D^2N}\right),\left(\frac{\sigma}{\rho}\right),\left(\frac{L}{D}\right),(J),(f),(e),(v),(u)(n)\right\} \quad \textbf{(EQ 61)}$$

where

- P = power
- D = internal diameter of the mill
- N = speed of rotation of the mill, rps
- ρ = density of ball material
- ϕ = denotes some function of each of the dimensionless groups
- h = height of lifters
- d = diameter of the balls
- g = acceleration due to gravity
- b = representative particle dimension
- H = energy required to bring about unit increase in the specific surface of the powder (specific surface in units of area per unit mass)
- ν = kinematic viscosity of the mixture of powder and fluid
- σ = effective density of the mixture of powder and fluid
- L = internal length of the mill
- J = volume occupied by the ball charge (including voids), expressed as a fraction of the mill volume
- f = coefficient of friction between balls and the mill
- e = coefficient restitution between the balls and the mill
- v = volume occupied by the powder charge (including voids), expressed as a fraction of the volume of voids in the ball charge
- u = volume occupied by fluid expressed as a fraction of the volume of voids in the charge
- n = number of lifters

Following analysis of their experimental results, they arrived at the following equation:

$$P = D^5N^3\rho_b\left(1 + 0.4\frac{\rho_p}{\rho_b}\right)\left(\frac{L}{D}\right)\times\gamma_1\left(\frac{N_c}{N}\right)\times\gamma_2(J) \times\gamma_3\left(\frac{D}{d}\right)\times\gamma_4(n)\times\gamma_5\left(\frac{h}{D}\right) \quad \textbf{(EQ 62)}$$

where N_c is the critical speed of rotation of the mill. The functions γ_1–γ_5 were fitted to their laboratory mill data and were presented in graphical form. The functions γ_3–γ_5 were found to be equal to unity for most conditions. The function γ_1 was approximated by them as

$$\gamma_1\left(\frac{N_c}{N}\right) = 3.13\phi^{-2} \quad \textbf{(EQ 63)}$$

where ϕ is the fraction of critical speed.

The function γ_2 was fitted by Morrell (1993) to Rose and Evans' data to give the following equation:

$$\gamma_2(J) = 3.3506J_t + 1.3372J_t^2 - 9.1602J_t^3 \quad \textbf{(EQ 64)}$$

The effect of the discharge type was also addressed by Rose and Evans through the application of an additional function (γ_6), which the product of Equation 62 was multiplied by. Again, the function was presented in graphical form. This function was also fitted by the author as follows:

$$\gamma_6 = 1.7796 - 6.2164J_t + 13.6615J^2 - 8.1923J^3 \quad \textbf{(EQ 65)}$$

Rose and Evans developed their model for ball mills and therefore their charge density (ρ_b) is in terms of the specific gravity of steel. To modify their equation to apply to SAG and AG mills, the ρ_b term was replaced by the mean density of the grinding media (ρ_c) as follows:

$$\rho_c = \frac{J_b\rho_b + J_o\rho_o}{J_t} \quad \textbf{(EQ 66)}$$

where

J_b = volume of mill occupied by ball component of grinding media (including voids)
J_o = volume of mill occupied by ore component of grinding media (including voids)
ρ_o = ore specific gravity
J_t = volume of mill occupied by total grinding charge ($J_t = J_b + J_o$)

For ball mills, where $J_o = 0$ and $J_b = J_t$, Equation 66 reduces to $\rho_c = \rho_b$.

Validation

The mill power draw database that was published by Morrell (1993) and is reproduced in Tables 2–4 was used to evaluate the Rose and Evans power draw model. Results are shown graphically in Figures 50 and 51. Statistical analysis of results shows that for ball mills, the standard deviation of the differences between observed and predicted values is 6.3% with an overall mean of differences of 15.0%. For AG/SAG mills, the associated figures are 9.0% and 27.1%, respectively. The results indicate there is considerable bias of the prediction of AG/SAG mill power draw. However, if this could be corrected, the standard deviation results indicate that it would be better than Austin, Bond, and Harris et al.'s models. For ball mills, the Rose and Evans model also has some bias, and if this could be corrected, it would be on par with Bond's ball mill model.

Morrell Model

Morrell (1993) used an energy balance approach where power was taken to be the rate at which potential and kinetic energy is imparted to the charge. He used a different shape of the charge from that given in Figure 40, opting instead for the one shown in Figure 52.

Morrell argued that this more accurately described the shape of the moving charge in contact with the mill shell (i.e., it excluded material in flight and the stationary material at the

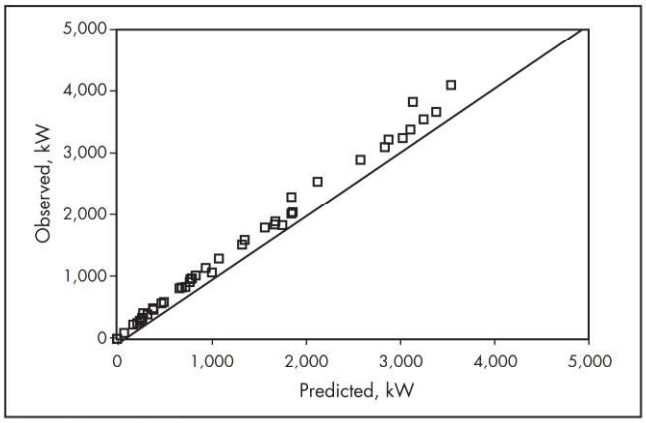

Source: Morrell 1993

Figure 50 Observed versus predicted power draw of ball mills using the Rose and Evans model

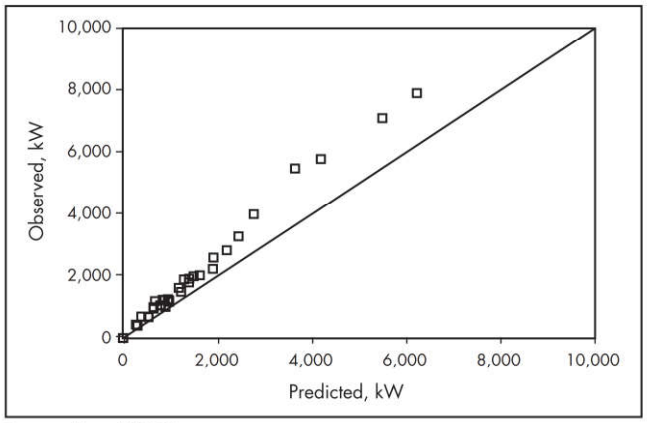

Source: Morrell 1993

Figure 51 Observed versus predicted power draw of AG/SAG mills using the Rose and Evans model

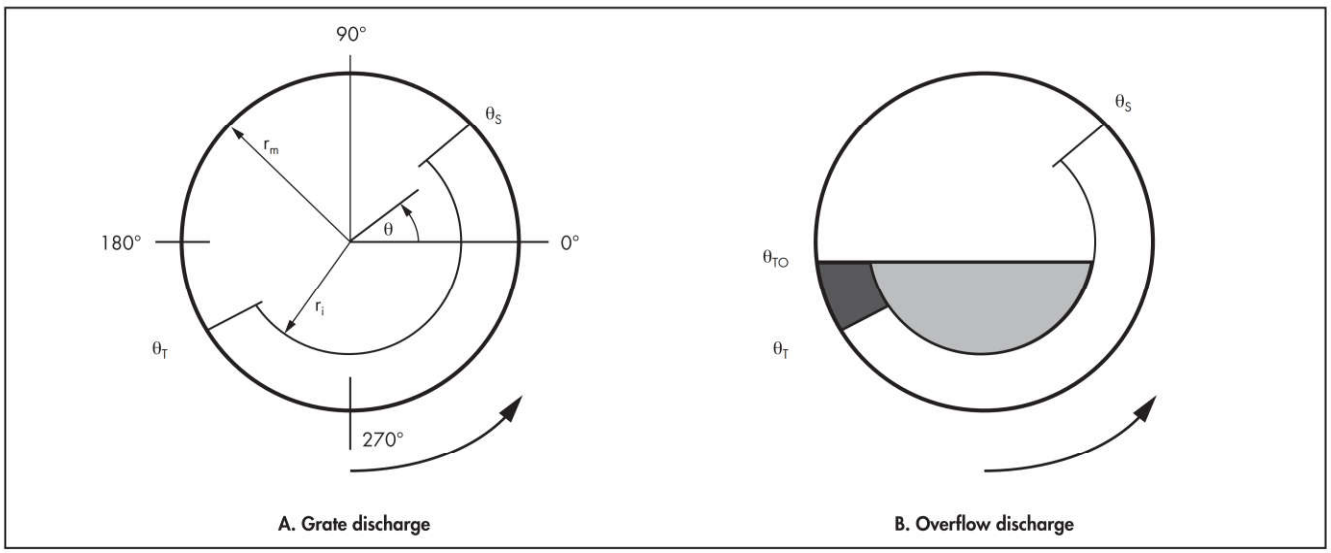

Figure 52 (A) Simplified charge shape for grate mills (no slurry pool); (B) simplified charge shape for overflow mills

center of the charge). These conclusions came from observations of the shape of the charge in a glass laboratory mill (Figure 53).

Equation 67 was therefore developed for the cylindrical section of the mill (a similar equation was also developed for conical ends). From this equation, the power associated with the rock/ball charge is calculated separately from the slurry, the total power being the sum of both.

$$P_{cylinder} = \int_{r_i}^{r_m} \left(V_r L r g \begin{pmatrix} \rho_c(\sin\theta_S - \sin\theta_T) \\ +\rho_p(\sin\theta_S - \sin\theta_{Tp}) \end{pmatrix} \right) dr \qquad \textbf{(EQ 67)}$$

where

$P_{cylinder}$ = power delivered to the charge (net power)
r_m = radius of mill inside liners
r_i = radial position of charge inner surface
V_r = tangential velocity of a particle at radial distance r
L = length of cylindrical section of the mill inside liners
r = radial position
g = gravitational constant
ρ_c = density of rock/ball charge (excluding pulp)
θ_S = angular displacement of shoulder position at the mill shell
θ_T = angular displacement of the grinding media toe position at the mill shell
ρ_p = density of pulp phase
θ_{Tp} = angular displacement of the slurry toe position at the mill shell. For overflow ball mills and AG/SAG mills with slurry pooling, $\theta_{Tp} = \theta_{TO}$ (see Figure 52B).

Equation 67 shows that to execute the model, it is necessary to also have relationships that predict values for parameters such as θ_S, θ_T, θ_{Tp}, θ_{TO}, V_r, ρ, and r_i. All of these relationships are provided by Morrell (1993, 1996a).

Equation 67 describes the power draw by the charge (net power). It does not include electrical losses across the motor as well as the power required to overcome friction in the bearings, and losses in gearboxes/reducers as well as in the gear/pinion coupling, where the mill has a gear-and-pinion drive. Note that this definition of *net power* is not the same as the definition of "power at pinion." The power at pinion cannot normally be measured other than in some pilot mills and is estimated from assumptions about the energy losses of various components in the drive train. Theoretically, it is the power delivered to the pinion shaft in gear-and-pinion drives. It is meant to account for electrical motor and gearbox/reducer energy losses only but does not include the energy losses associated with the pinion gear/ring gear coupling nor bearings.

In practice, the only power draw that is usually measured in full-scale plants is the metered power (i.e., motor input power). Given this fact, and the need to properly validate the model through comparison of measured and predicted values, the power model must also predict motor input power. To do so, the model is configured as follows:

$$\text{motor input power} = \text{no-load power} + \text{net power} \qquad \textbf{(EQ 68)}$$

Net power is given by Equation 67. A further equation that predicts no-load power is required. The semi-empirical no-load power equation form proposed by Morrell (1996a) is used for this purpose, though it has been modified slightly based on additional data:

$$\text{no-load power (kW)} = K(D^{2.5}\phi(0.667L_d + L))^{0.82} \qquad \textbf{(EQ 69)}$$

where

K = 2.13 for gear and pinion drives and 1.28 for gearless drives
D = mill diameter
ϕ = fraction of critical speed
L_d = length of cone end
L = length of cylindrical section

The resultant model should be applicable to all tumbling mills.

Source: Morrell 1993
Figure 53 Charge inside a rotating mill

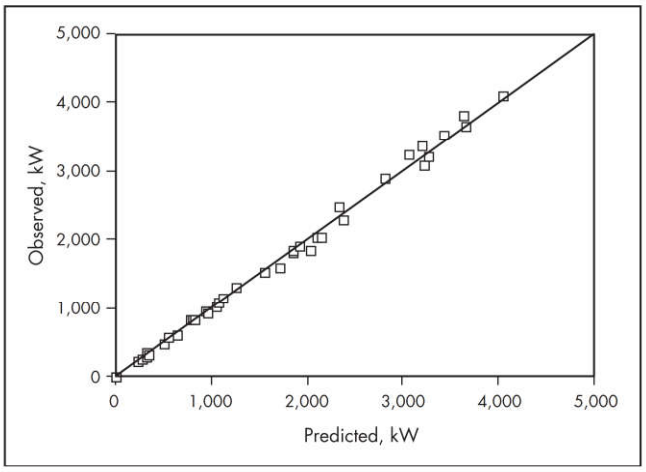

Source: Morrell 1993
Figure 54 Observed versus predicted power draw of ball mills using the Morrell model

Validation

The mill power draw database that was published by Morrell (1993) and is reproduced in Tables 2–4 was used to evaluate

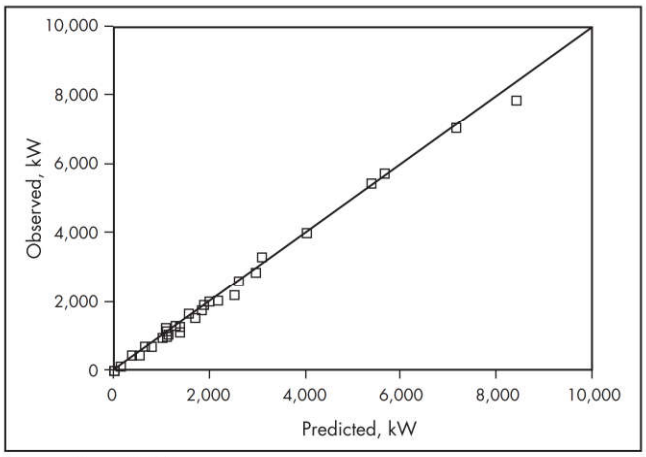

Source: Morrell 1993

Figure 55 Observed versus predicted power draw of AG/SAG mills using the Morrell model

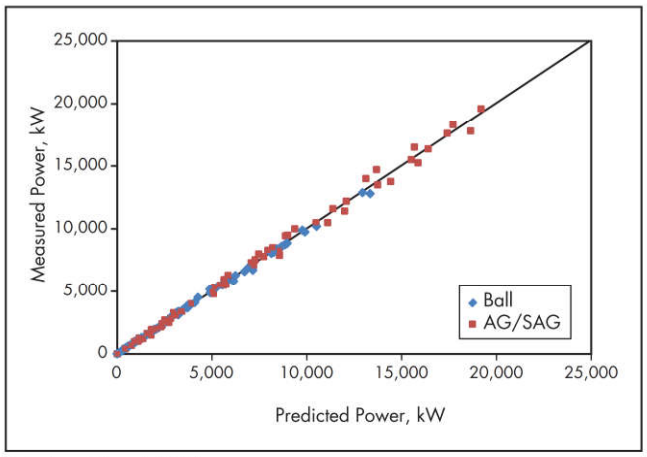

Data from Morrell 2004a

Figure 56 Observed versus predicted power draw of 140 AG, SAG, and ball mills using Morrell power model

the Morrell power draw model. Results are shown graphically in Figures 54 and 55. Statistical analysis of results shows that for ball mills, the standard deviation of the differences between observed and predicted values is 4.4% with an overall mean of differences of 0.3%. For AG/SAG mills, the associated figures are 6.3% and 0.4%, respectively.

Morrell added to his 1993 published database and used it to further benchmark his model (Morrell 2004a), the results of which are illustrated in Figure 56. The data comprise more than 140 ball, AG, and SAG mill data sets. The standard deviation of the differences between ball mill observed and predicted values is 3.1% with an overall mean of difference of 0.0%. For AG/SAG mills, the associated values are 3.8% and 0.0%, respectively.

Power Draw Data

The only comprehensive database of mill power draws and associated mill design and operating conditions that has been published to date is that accumulated by Morrell (1993, 1996b). The details of this database are in Tables 2–4.

In relation to the power draw data that the tables contain, operating plants vary widely in the type and complexity of their instrumentation. As a result, power draw data can be available on-site from a range of devices including kilwatt hour meters, power transducers, and ammeters. Where more than one source of power data was available at a particular site, it was ensured that all sources gave similar readings. If they did not give similar readings, plant electrical staff were asked to investigate and correct the differences. Where this could not be done, the data were not included in the database. If only one source of power measurement was available, efforts were made to ensure that independent checks of the power reading accuracy had been made either prior to the field study or shortly afterward.

The comments in the preceding paragraph are particularly relevant when using some published sources of power draw information, where appropriate checks of the power draw measurements have not been carried out because they may contain significant inaccuracies.

Additional, although limited, data that has been sourced from other published sources can be found in Doll (2013) together with an evaluation of Austin'sand Morrell's model. Daniel et al. (2010) also provide an assessment of the Austin, Hogg and Fuerstenau, and Morrell models.

STEEL WEAR PREDICTION

The most popular laboratory wear test to date is the one developed by Bond (1961). The test machine comprises a drum rotating at 70 rpm into which a sample of ore to be tested is introduced. Also in the drum is a rotating steel impeller comprising a steel paddle with dimensions 3 × 1 × 0.25 in., its center of rotation the same as the drum. The impeller rotates at 632 rpm, and as the drum rotates, the impeller is showered with rock pieces. As a result, the impeller is worn down.

The standard test uses a total of 1.6 kg of rock sample, in the size range –0.75+0.5 in. The 1.6 kg total is divided into four equal batches of 400 g and each batch is placed in the machine for 15 minutes, then removed. The total weight loss (g) of the paddle that results is determined, and this weight loss is designated Ai, the abrasion index.

Equations

Rowland (1982) provides the following equations for applying the abrasion index:

Wet rod mills:

$$\text{rod wear} = 0.159\ (\text{Ai} - 0.020)^{0.2}\ \text{kg/kW·h} \qquad \textbf{(EQ 70)}$$

$$\text{liner wear} = 0.0159\ (\text{Ai} - 0.015)^{0.3}\ \text{kg/kW·h} \qquad \textbf{(EQ 71)}$$

Wet ball mills:

$$\text{ball wear} = 0.159\ (\text{Ai} - 0.015)^{0.34}\ \text{kg/kW·h} \qquad \textbf{(EQ 72)}$$

$$\text{liner wear} = 0.0118\ (\text{Ai} - 0.015)^{0.3}\ \text{kg/kW·h} \qquad \textbf{(EQ 73)}$$

For AG/SAG mills, Giblett and Seidel (2011) proposed the following equation from their analysis of a range of measured wear data from Newmont circuits:

$$\text{SAG mill ball wear} = 0.0017(\text{A} \times \text{b}) - 0.0074 \qquad \textbf{(EQ 74)}$$

where A and b are the JK comminution modeling parameters that are obtained from SMC Tests/drop weight tests.

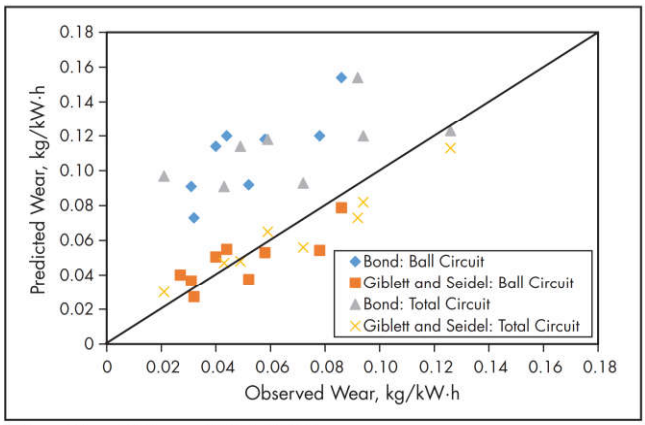

Adapted from Giblett and Seidel 2011

Figure 57 Predicted versus observed ball wear rates

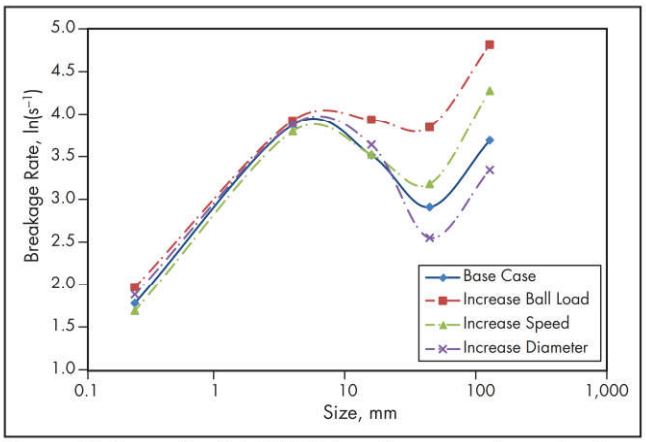

Figure 58 Example of AG/SAG breakage rate dependencies

For ball mills, Giblett and Seidel proposed the following:

$$\text{ball mill ball wear} = 0.0817(\text{Ai})^{0.498} \quad \textbf{(EQ 75)}$$

Validation

The only significant data that have been published are those of Giblett and Seidel (2011). These are plotted in Figure 57 and show that the Giblett and Seidel equations predict the observed wear rates quite well and are far superior to Bond/Rowland's equations.

PROCESS SIMULATION MODELING

The advent and rapid development of high-speed computers provided the opportunity to develop complex models of comminution machines that could execute their calculations very rapidly and could be linked together such that entire circuits could be simulated. These models contrast significantly with the energy–size relationships and are aimed at reproducing the overall response of comminution machines in terms of throughput, power draw, and product size distribution. By their nature, such models are relatively complex and may have many interactions between the various subprocesses that describe the machine in question, and that without computers would be almost impossible to apply in a reasonable time frame. Therefore, in parallel with the development of modern computers, researchers started developing mathematical simulation models of AG/SAG mills, ball mills, crushers, and classifiers (Lynch 1977; Austin et al. 1984; Herbst and Fuerstenau 1973; Whiten 1974). Much of the early modeling work was academically oriented and of little benefit to practicing metallurgists. However, as time went on, user-friendly interfaces were developed that broadened the models' appeal and impact. Such developments gave rise to process simulators such as MODSIM, USIM PAC, METSIM, and JKSimMet.

In all cases, comminution simulation model researchers relied on what is known as the population balance model (or variants of it) as their mathematical framework because it elegantly encapsulated the size reduction process in many comminution machines. The population balance model was originally introduced by Epstein (1947) and can be represented as follows:

$$0 = f_i - p_i + \sum_{j=1}^{i-1} k_j s_j b_{ij} - k_i s_i \quad \textbf{(EQ 76)}$$

where

f_i = t/h of particles of size i in the feed
p_i = t/h of particles of size i in the product
b_{ij} = breakage distribution function
k_i = breakage rate of particles of size i
s_i = mass of particles in the charge of size i

Whiten's (1974) variant of the population balance model essentially uses Equation 76, but to it he added another equation that enabled the introduction of material transportation to be easily incorporated, which greatly aided the development of grate discharge mill models such as those that could be applied to AG/SAG mills. This equation was written:

$$p_i = d_i s_i \quad \textbf{(EQ 77)}$$

where d_i is the discharge rate of particles of size i.

The simplicity of the preceding equations is the source of both their greatest strengths and their greatest weakness. Their greatest strengths are their ease of use and versatility, while their greatest weakness is the lack of any physical description of the subprocesses on which they depend. For them to be used successfully, therefore, a series of supplementary models must be developed and linked to them. Even when such subprocesses are developed, invariably there will remain a range of parameters that must be specified for the models to work. Considering Equations 76 and 77, for example, if a product size distribution and charge must be obtained from simulation of a mill grinding a specified feed, then size-distributed parameters k_i, b_i, and d_i must be specified. In the case of the JKSimMet modeling approach (Napier-Munn et al. 1996), the b_i parameters were derived from the A and b values that are obtained from drop weight or SMC Tests. This left the d_i and k_i, which, in the early years of development, had to be fitted to data from existing mills. Consequently, the use of such models was restricted to process optimization studies, and therefore in design situations they were of limited use. However, even though limited to optimization studies, such models were extremely valuable because they enabled practicing metallurgists to run and assess strategies to improve plant performance. This significantly reduced the time-consuming and potentially costly trial-and-error field experimentation that was the usual methodology until then.

Many models in currently commercially available simulators still suffer from the problem of requiring existing plant

data for suitable parameters and therefore still have limited use in design projects. The JKSimMet AG/SAG mill variable rates model (Morrell and Morrison 1996) and Morrell's (2004c) model are two exceptions. Both models used a range of operating plant data to determine the dependency of the model parameters on factors such as mill design and operating conditions. An example of the data that was used to develop these dependencies is shown in Figure 58. It illustrates the highly important breakage rate distribution, which changes its shape depending on the design and operating conditions. By mathematically describing how this shape changes, the resultant equations can be used in design situations to predict all of the required parameters for the simulation to be performed. This gives the design metallurgist a very powerful tool because it enables stream mass and size balances to be generated from the chosen circuit and chosen mill sizes, and allows him or her to run sensitivity analyses to ensure that target throughputs and grind sizes can be achieved under a range of feed and operating conditions. It significantly increases confidence that the chosen circuit and equipment will achieve their specified goals.

No model (regardless of how sophisticated) is an expert system that enables metallurgists with limited knowledge/experience to become "instant experts" by having a simulator at their disposal. Models/simulators are just tools, and it is incumbent on the user to fully understand how they work, what their limitations are, and the operational intricacies of the processes that they simulate. Knowing the model's limitations is particularly important, and this can only be established by benchmarking the model's performance over as wide a range of operating data as possible. According to the published literature, this benchmarking has not often been done, with the exception of the JKMRC variable rates model (Morrell and Morrison 1996) and Morrell model (Morrell 2004c).

REFERENCES

Amelunxen, P. 2003. The application of the SAG power index to ore body hardness characterization for the design and optimization of autogenous grinding circuits. Master of Engineering thesis, McGill University, Canada.

Amelunxen, P., Berrios P., and Rodriguez, E. 2014. The SAG grindability index. *Miner. Eng.* 55:42–51.

Amelunxen, P., De la Cruz, R., Berrios, P., and Panduro, L. 2016. Revisión Tecnica del SAG Grindability Index (SGI and MiniSGI). Presented at 2nd International Seminar on Geometallurgy (GEOMET2016), Gecamin, Lima, Peru.

Angove, J.E., and Dunne, R.C. 1997. A review of standard physical ore property determinations. Presented at the World Gold Conference, Singapore, September 1–3.

Austin, L.G. 1990. A mill power equation for SAG mills. *Miner. Metall. Process*. (February):57–63.

Austin, L.G., Klimpel, R.R., and Luckie, P.T. 1984. *The Process Engineering of Size Reduction: Ball Milling*. New York: AIME.

Bailey, C., Lane, G., Morrell, S., and Staples, P. 2009. What can go wrong in comminution circuit design? Presented at the Tenth Mill Operators' Conference, Adelaide, South Australia, Australia, October 12–14, 2009.

Barratt, D.J., and Allan, M.J. 1986. Testing for autogenous and semiautogenous grinding: A designer's point of view. *Miner. Metall. Process*. 3:65–74.

Blaskett, K.S. 1969. Estimation of the power consumption in grinding mills. In *Proceedings of the Ninth Commonwealth Mining and Metallurgy Congress*, Vol. 3. London: Institution of Mining and Metallurgy. pp. 631–649.

Bond, F.C. 1946. Crushing tests by pressure and impact. *Trans. AIME* 169:58–65.

Bond, F.C. 1952. The third theory of comminution. *Trans. AIME* 193:484–494.

Bond, F.C. 1960. Confirmation of the third theory. *Trans. AIME* 217:139–153.

Bond, F.C. 1961. *Crushing and Grinding Calculations*. Milwaukee, WI: Allis-Chalmers Manufacturing.

Bond, F.C. 1962. *Crushing and Grinding Calculations Additions and Revisions*. Milwaukee, WI: Allis-Chalmers Manufacturing.

Bond, F.C. 1963. Metal wear in crushing and grinding. Presented at the 54th Annual Meeting of the American Institute of Chemical Engineers.

Bond, F.C., and Maxon, W. 1943. *Standard Grindability Tests and Calculations*. New York: AIME.

Daniel, M., Lane, G., and Morrell, S. 2010. Consolidation and validation of several tumbling mill power models. Presented at Procemin 2010, Santiago, Chile.

Dobby, G., Bennett, C., and Kosick, G. 2001. Advances in SAG circuit design and simulation applied to the Mine Block Model. In *Proceedings of the Conference on International Autogenous and Semi-Autogenous Grinding Technology 2001*. Vol. 4. Vancouver, BC: Mining and Mineral Process Engineering, University of British Columbia.

Doll, A. 2013. A comparison of SAG mill models. Presented at Procemin 2013, Santiago, Chile.

Epstein, B. 1947. The material description of certain breakage mechanisms leading to the logarithmic-normal distribution. *J. Franklin Inst*. 244:471–477.

Flavel, M.D., and Rimmer, H.W. 1982. Particle breakage studies in an impact environment. SME Preprint No. 82-124. Littleton, CO: SME.

Forsund, B., Norkyn, I., Sankvik, K.L., and Winther, K. 1988. Sydvarangers 6.5m diameter × 9.65m ball mill. In *Proceedings of the XVI International Mineral Processing Congress*. Edited by K.S.E. Forssberg. New York: Elsevier. pp. 171–183.

Giblett, A., and Morrell, S. 2016. Process development testing for comminution circuit design. *Miner. Metall. Process.* 33(4):172.

Giblett, A., and Seidel, J. 2011. Measuring, predicting and managing grinding media wear. Paper No. 34. In *Proceedings of the Conference on International Autogenous and Semi-Autogenous Grinding Technology 2011*. Vancouver, BC: Mining and Mineral Process Engineering, University of British Columbia.

Harris, C.C., Schnock, E.M., and Arbiter N. 1985. Grinding mill power consumption. *Miner. Process. Tech. Rev.* 1:297–345.

Herbst, L.A., and Fuerstenau, D.W. 1973. Mathematical simulation of dry ball milling using specific power information. *Trans. AIME* 254:343–348.

Hogg, R., and Fuerstenau, D.W. 1972. Power relationships for tumbling mills. *Trans. AIME* 252: 418–423.

Kosick, G.A., and Bennett, C. 1999. The value of ore body power requirement profiles for SAG circuit design. In *Proceedings of the 31*st *Annual Meeting of the Canadian Mineral Processors*, Ottawa, ON: Canadian Mineral Processors.

Lane, G.S. 2010. What is a competent ore and how does this effect comminution circuit design? In *Proceedings of the 7th International Mineral Processing Conference—Procemin 2010.* Santiago, Chile: Gecamin.

Lane, G., Foggiatto, B., and Bueno, M. 2013. Power-based comminution calculations using Ausgrind. Presented at Procemin 2013, Santiago, Chile.

Leung, K. 1987. An energy-based ore specific model for autogenous and semi-autogenous grinding. Ph.D. thesis, Julius Kruttschnitt Mineral Research Centre, University of Queensland, Australia.

Lynch, A.J. 1977. *Mineral Crushing and Grinding Circuits: Their Simulation, Optimisation, Design and Control.* Amsterdam, Netherlands: Elsevier Scientific.

MacPherson, A.R., and Turner, R.R. 1978. Autogenous grinding from test work to purchase of a commercial unit. In *Mineral Processing Plant Design, Practice, and Control*. Edited by A.L. Mular and R.B. Bhappu. New York: AIME. pp. 279–305.

Matei, V., Bailey, C.W., and Morrell, S. 2015. A new way of representing A and B parameters from JK drop-weight and SMC Tests: The "SCSE." Paper No. 16. In *Proceedings of the Conference on International Autogenous and Semi-Autogenous Grinding Technology 2015*. Vancouver, BC: Mining and Mineral Process Engineering, University of British Columbia.

Moore, D.C. 1982. Prediction of crusher power requirements and product size analysis. In *Design and Installation of Comminution Circuits*. Edited by A.L. Mular. New York: AIME. pp. 218–227.

Morrell, S. 1993. The prediction of power draw in wet tumbling mills. Ph.D. thesis, University of Queensland, Australia.

Morrell, S. 1996a. Power draw of wet tumbling mills and its relationship to charge dynamics—Part 1: A continuum approach to mathematical modelling of mill power draw. *Trans. Inst. Min. Metall.* 105:C43–C53.

Morrell, S. 1996b. Power draw of wet tumbling mills and its relationship to charge dynamics—Part 2: An empirical approach to modeling of mill power draw. *Trans. Inst. Min. Metall.* 105:C54–C62.

Morrell, S. 2001. Large diameter SAG mills need large diameter ball mills—What are the issues? In *Proceedings of the Conference on International Autogenous and Semi-Autogenous Grinding Technology 2001.* Vancouver, BC: Mining and Mineral Process Engineering, University of British Columbia.

Morrell, S. 2004a. Predicting the specific energy of autogenous and semi-autogenous mills from small diameter drill core samples. *Miner. Eng.* 17(3):447–451.

Morrell, S. 2004b. An alternative energy-size relationship to that proposed by bond for the design and optimisation of grinding circuits. *Int. J. Miner. Process*. 74:133–141.

Morrell, S. 2004c. A new autogenous and semi-autogenous mill model for scale-up, design, and optimisation. *Miner. Eng.* 17(3):437–445.

Morrell, S. 2009. Predicting the overall specific energy requirement of crushing, high pressure grinding roll and tumbling mill circuits. *Miner. Eng.* 22(6):544–549.

Morrell, S. 2010. Predicting the specific energy required for size reduction of relatively coarse feeds in conventional crushers and high pressure grinding rolls. *Miner. Eng.* 23(2):151–153.

Morrell, S. 2011a. The appropriateness of the transfer size in AG and SAG mill circuit design. Paper No. 153. In *Proceedings of the Conference on International Autogenous and Semi-Autogenous Grinding Technology 2011.* Vancouver, BC: Mining and Mineral Process Engineering, University of British Columbia.

Morrell, S. 2011b. Mapping orebody hardness variability for AG/SAG/crushing and HPGR circuits. Paper No. 154. In *Proceedings of the Conference on International Autogenous and Semi-Autogenous Grinding Technology 2011.* Vancouver, BC: Mining and Mineral Process Engineering, University of British Columbia.

Morrell, S., and Morrison, R. 1996. AG and SAG mill circuit selection and design by simulation. In *Proceedings of the Conference on International Autogenous and Semi-Autogenous Grinding Technology 1996*. Vancouver, BC: Mining and Mineral Process Engineering, University of British Columbia. pp. 769–790.

Mosher, J.B., and Bigg, A.C.T. 2001. SAG mill test methodology for design and optimization. In *Proceedings of the Conference on International Autogenous and Semi-Autogenous Grinding Technology 2001.* Vancouver, BC: Mining and Mineral Process Engineering, University of British Columbia.

Mosher, J.B., and Tague, C.B. 2001. Conduct and precision of bond grindability testing. *Miner. Eng.* 14(10):1187–1197.

Napier-Munn, T.J., Morrell, S., Morrison, R.D., and Kojovic, T. 1996. *Mineral Comminution Circuits: Their Operation and Optimisation*. Indooroopilly, Queensland: Julius Kruttschnitt Mineral Research Centre, University of Queensland, Australia.

Narayanan, S.S., and Whiten, W.J. 1988. Determination of comminution characteristics from single particle breakage tests and its application to ball mill scale-up. *Trans. Inst. Min. Metall.* 97:C115–C124.

Oestreicher, C., and Spollen, C.F. 2006. HPGR vs SAG Mill Selection for the Los Bronces Grinding Circuit expansion. In *Proceedings of the Conference on International Autogenous and Semi-Autogenous Grinding Technology 2006.* Vancouver, BC: Mining and Mineral Process Engineering, University of British Columbia. pp. 110–123.

Rayo, J. 2014. Comparison of semi-autogenous mills operations in Andean countries. In *Proceedings of the 12th AusIMM Mill Operators Conference*. Townsville, Queensland, Australia. pp. 283–295.

Rose, R.E., and Blunt, G.D. 1956. The dynamics of the ball mill, Part III: An investigation into the surging of ball mills. *Proc. Inst. Mech. Eng.* 170(1):793–800.

Rose, H.E., and Evans, D.E. 1956a. The dynamics of the ball mill, part I: Power requirements based on the ball and shell system. *Proc. Inst. Mech. Eng.* 170(1):773–783.

Rose, H.E., and Evans, D.E. 1956b. The dynamics of the ball mill, part II: The influence of the powder charge on power requirements. *Proc. Inst. Mech. Eng.* 170(1):784–792.

Rowland, C.A., Jr. 1972. *Grinding Calculations Related to the Application of Large Rod and Ball Mills*. Allis-Chalmers Publication 22P4704. Milwaukee, WI: Allis-Chalmers Manufacturing.

Rowland, C.A., Jr. 1973. Comparison of work indices calculated from operating data with those from laboratory test data. In *Proceedings of the 10th Commonwealth Mining and Metallurgy Congress*, Ottawa, ON, Canada. pp. 47–61.

Rowland, C.A., Jr. 1982. Selection of rod mills, ball mills, pebble mills and regrind mills. In *Design and Installation of Comminution Circuits*. Edited by A.L. Mular and G.V. Jergensen. New York: AIME. pp. 393–438.

Rowland, C.A., Jr., and Kjos, D.M. 1978 (revised 1980). Rod and ball mills. In *Mineral Processing Plant Design, Practice, and Control*. Edited by A.L. Mular and R.B. Bhappu. New York: AIME. pp. 239–278.

Scinto, P., Festa, A., and Putland, B. 2015. OMC Power-based comminution calculations for design, modelling and circuit optimization. In *Proceedings of the 47th Annual Meeting of the Canadian Mineral Processors*. Ottawa, ON: Canadian Mineral Processors.

Shi, F., Lambert, S., and Daniel, M. 2006. A study of the effects of HPGR treating platinum ores. In *Proceedings of the Conference on International Autogenous and Semi-Autogenous Grinding Technology 2006.* Vancouver, BC: Mining and Mineral Process Engineering, University of British Columbia. pp. 154–171.

Starkey, J., and Dobby, G. 1996. Application of the Minnovex SAG Power Index at five Canadian SAG plants. In *Proceedings of the Conference on International Autogenous and Semi-Autogenous Grinding Technology 1996.* Vancouver, BC: Mining and Mineral Process Engineering, University of British Columbia. pp. 110–123.

Starkey, J., and Larbi, K. 2012. SAGDesign—Using open technology for mill design and performance assessments. Presented at Procemin 2012, Santiago, Chile.

Starkey, J., Dobby, G., and Kosick, G. 1994. A new tool for SAG hardness testing. In *Proceedings of the 26th Canadian Mineral Processors Annual Meeting*. Ottawa, ON: Canadian Mineral Processors.

Starkey, J., Hindstrom, S., and Nadasdy, G. 2006. SAGDesign testing—What it is and why it works. In *Proceedings of the Conference on International Autogenous and Semi-Autogenous Grinding Technology 2006*. Vancouver, BC: Mining and Mineral Process Engineering, University of British Columbia. pp. 240–254.

Steane, R.A., and Hinckfuss, D.A. 1979. Selection and performance of large diameter ball mills at Bougainville Copper Ltd. Papua New Guinea. In *Proceedings of the 11th Commonwealth Minerals and Metallurgy Congress*. Hong Kong. pp. 577–584.

Stephenson, I. 1997. The downstream effects of high pressure grinding rolls processing. Ph.D. thesis, Julius Kruttschnitt Mineral Research Centre, University of Queensland, Australia.

Whiten, W.J. 1974. A matrix theory of comminution machines. *Chem. Eng. Sci.* 29:588–599.

PART 4

Classification and Washing